Progress of Theoretical Physics, Vol. 112, No. 3, September 2004

New Numerical Methods to Evaluate Homogeneous Solutions of the Teukolsky Equation

Ryuichi Fujita and Hideyuki Tagoshi

Department of Earth and Space Science, Graduate School of Science, Osaka University, Toyonaka 560-0043, Japan

(Received June 24, 2004)

We discuss a numerical method to compute the homogeneous solutions of the Teukolsky equation which is the basic equation of the black hole perturbation method. We use the formalism developed by Mano, Suzuki and Takasugi, in which the homogeneous solutions of the radial Teukolsky equation are expressed in terms of two kinds of series of special functions, and the formulas for the asymptotic amplitudes are derived explicitly. Although the application of this method was previously limited to the analytical evaluation of the homogeneous solutions, we find that it is also useful for numerical computation. We also find that so-called "renormalized angular momentum parameter", ν, can be found only in the limited region of ω for each l, m if we assume ν is real (here, ω is the angular frequency, and l and m are degree and order of the spin-weighted spheroidal harmonics respectively). We also compute the flux of the gravitational waves induced by a compact star in a circular orbit on the equatorial plane around a rotating black hole. We find that the relative error of the energy flux is about 10^{-14} which is much smaller than the one obtained by usual numerical integration methods.

§1. Introduction

Inspirals of stellar-mass compact objects into a supermassive black hole at galactic nuclei are expected to be one of the most important sources of the gravitational waves for space-based detectors, such as the Laser Interferometer Space Antenna (LISA).[1] Current best estimate of the number of such event is given by Gair et al.[2] They estimated the number of event for the inspirals of $10M_\odot$ black holes into $10^6 M_\odot$ supermassive black holes to be 660 by 3 years observation. By observing gravitational waves from such systems, we may be able to obtain information of the central black hole's spacetime geometry encoded in multipole moments, and test the validity of the no-hair theorem of black hole.[3] We may also obtain astrophysical information such like the mass distribution of compact objects in galactic nuclei. The optimal detection strategy for such gravitational waves is matched filtering, which requires theoretical waveforms to be correlated with the data. Although we may not need very accurate waveforms in detection, we will need very accurate theoretical waveforms to extract astrophysical information concerning the source.

To predict the waveforms of extreme mass ratio inspirals, we adopt the black hole perturbation approach. In this approach, a compact star is treated as a point particle, and the mass of the compact star, μ, is assumed to be very small compared to the mass of the black hole, M, i.e. $\mu/M \ll 1$. In this context, the Teukolsky equation[4] describes the evolution of a perturbation of the Kerr black hole spacetime. The standard approach to solve the Teukolsky equation is based on the Green function

method. The Green function is constructed using two kinds of homogeneous solutions. The solution of the Teukolsky equation is obtained by integrating the Green function multiplied by the source term. In the case of a Kerr black hole, the homogeneous solution is calculated usually by the Sasaki-Nakamura equation,[5] which is derived with the Sasaki-Nakamura transformation from the Teukolsky equation. The Sasaki-Nakamura transformation is a generalization of the Chandrasekhar transformation[6] by which we can obtain the Regge-Wheeler equation from the Bardeen-Press-Teukolsky equation[4),7] in the Schwarzschild case. The Sasaki-Nakamura equation is also a powerful formula when we compute the gravitational wave flux induced by particles in unbound orbits.

In the past, there were several works which calculated the flux and waveforms of gravitational waves induced by a compact star around a black hole computed by the Teukolsky and the Sasaki-Nakamura equations, and its effects to the orbital evolution of the star under the influence of radiation reaction. Here, we list some of recent works treating bound orbits of the star. Many other works can also be found in a review article by Nakamura et al.[8]

Shibata[9] calculated the gravitational waves in the case of circular, equatorial orbits around a Kerr black hole. Finn and Thorne[10] consider the same case, and discussed the signal-to-noise ratio of such gravitational waves when detected by LISA and the detectability of such sources by LISA. Tanaka et al.[11] and Cutler et al.[12] calculated the gravitational waves in the case of eccentric orbits around a Schwarzschild black hole, and discussed orbital evolution of the star. Apostolatos et al.[13] consider the slightly eccentric orbits around a Schwarzschild black hole, and discussed the stability of the circular orbit under the influence of radiation reaction. Kennefick[14] consider the slightly orbits on the equatorial plane around a Kerr black hole, and discussed the stability of the circular orbit under the influence of radiation reaction. Shibata[15] calculated the gravitational waves in the case of eccentric, equatorial orbits around a Kerr black hole, and discuss the importance of the black hole spin and other relativistic effects. Glampedakis and Kennefick[16] calculated the gravitational waves in the case of eccentric, equatorial orbits around a Kerr black hole, and discuss the orbital evolution of the star under the influence of radiation reaction. Shibata[17] calculated the gravitational waves in the case of circular, nonequatorial orbits around a Kerr black hole, and discussed the radiation reaction effects. Hughes[18),19] calculated the gravitational waves in the case of circular, nonequatorial orbits around a Kerr black hole, and discuss the radiation reaction effects.

The source term of the Teukolsky equation is obtained by specifying the orbit of the particle. In the case of a Kerr black hole, orbits around it are specified by the energy, the z-component of the angular momentum, and the Carter constant. In the case of bound orbits, when the orbit is limited to the equatorial plane but is not circular, the orbits show exhibit the "zoom-whirl" property as the eccentricity becomes larger.[16] When the orbit is no longer limited to the equatorial plane, which may be important for sources of LISA, the orbits become more complicated. In such cases, we have to trace the orbit for much longer time than the dynamical time of the system in order to integrate the source term multiplied by the Green function accurately. Further, many side-bands in the spectrum of gravitational waves must

be calculated to establish the good accuracy.

Let us assume for simplicity that LISA will observe gravitational waves at the frequency $f \sim 10^{-2}$ Hz for one year. The total cycle of waves is typically $N_{\rm cycle} \sim 10^5$. Thus, the relative error for the luminosity $\Delta\dot{E}/\dot{E}$ required to establish the accuracy for the cycle, $\Delta N_{\rm cycle} \leq 1$ is $\Delta\dot{E}/\dot{E} \leq 10^{-5}$[20] in the simplest, circular orbit cases. For more complicated orbits, the requirement to the accuracy would be stronger than this. Although the accuracy, 10^{-5}, is already established in many of previous works, it would be very helpful for the future data analysis of LISA if we had more efficient and accurate methods to compute the homogeneous solutions of the Teukolsky equation to calculate the gravitational wave flux.

Among approaches to obtain homogeneous solutions of the Teukolsky equation, Leaver[21] formulated a method to express them in terms of a series of Coulomb wave functions. Although this series is convergent at the spatial infinity, it does not converge around the horizon. For this reason, it was suggested that a power series expansion around the horizon be used to obtain all of the asymptotic amplitudes of the homogeneous solution which are needed in the Green function. Using this method, Tagoshi and Nakamura[22] carried out a high precision computation of a homogeneous solution of the Teukolsky equation and obtained high precision numerical data of the gravitational wave flux induced by a particle in a circular orbit around a Schwarzschild black hole. In this calculation, the convergence of the series of Coulomb wave functions is very fast, and we can evaluate the series of Coulomb wave functions very accurately. Contrastingly, because the convergence of the power series expansion is very slow, it is not easy to evaluate it very accurately. In fact, the accuracy of the numerical data of the homogeneous solution is limited by the accuracy of the power series expansion.

Later, Mano, Suzuki and Takasugi (MST)[23] formulated a method to express a homogeneous solution in a series of hypergeometric functions around the horizon. This series has a very convenient property that allows it to be matched with the series of Coulomb wave functions around the infinity. Specifically, this property is that the three term recurrence relation among the expansion coefficients for the hypergeometric case is the same as that in Coulomb case. Owing to this property, it is possible to match the two series expansions analytically, and we can express the asymptotic amplitude of the homogeneous solution in terms of only the expansion coefficients, not in terms of the hypergeometric or Coulomb functions themselves. This property is that which distinguishes the MST method from the Leaver method. Because we do not need to use a power series expansion to determine the asymptotic amplitudes by numerical matching, it is expected that the matching can be done very efficiently in the MST method.

So far, the MST method has been used only in analytic calculations. There is a close relation between the Coulomb or hypergeometric series expansion and the low frequency expansion of the Teukolsky equation. Here, low frequency usually implies small post-Minkowskian or post-Newtonian expansion parameters. We can calculate the higher order terms of the post-Newtonian expansion of the gravitational wave flux from a black hole[24),25] systematically using this method. Tagoshi, Mano and

Takasugi[26] also computed the energy absorbed by a rotating black hole analytically assuming that the orbit of the particle is very large.

In this paper, we use the MST formalism for numerical computation of the homogeneous Teukolsky equation. We discuss the numerical method to calculate the homogeneous solutions in detail. One of the most important problem involving the MST formalism is to determine the so-called "renormalized angular momentum" ν by solving the equation $g(\nu) = 0$, which is expressed in terms of continued fractions. We investigate the numerical properties of this function $g(\nu)$. We find that, for each s, ℓ, m and q (s is the spin index of the Teukolsky equation, ℓ, m are the indices of the spin weighted spheroidal harmonics, and q is the Kerr parameter divided by the mass of black hole, $q = a/M$.), there is a maximum value of $M\omega$ for which we can find ν, assuming ν to be real. Because the applicability of the MST formalism depends on the existence of ν, this is a serious problem. Although our preliminary investigation suggests that we can find ν if we assume it to be complex, more effort is needed to establish the numerical accuracy. Therefore, we restrict the region of $M\omega$ for which we can find real ν.

Once we have the renormalized angular momentum ν, it is straightforward to evaluate the expansion coefficients and the series of hypergeometric functions or Coulomb wave functions. As expected, we find that the convergence of the series of hypergeometric functions and Coulomb wave functions is very fast, and we can evaluate the homogeneous solutions very accurately.

As a test calculation, we compute the gravitational wave flux induced by a particle in a circular orbit on the equatorial plane around a Kerr black hole. This is because that the numerical data for the energy flux can easily be compared with the one obtained by other methods. The accuracy of the numerical data is compared with that of previous works.

This paper is organized as follows. In §2, we review the Teukolsky formalism and the MST method. In §3, we discuss the numerical method to calculate the homogeneous solutions. We present numerical results of the gravitational wave flux induced by a particle in circular, equatorial orbits around a Kerr black hole in §3.5. Section 4 is devoted to a summary and discussion. Throughout this paper, we use units in which $G = c = 1$.

§2. Analytic solutions of the homogeneous Teukolsky equation

2.1. *The homogeneous solutions in series of hypergeometric functions and Coulomb wave functions*

The radial Teukolsky equation is given by (see Appendix A)

$$\Delta^2 \frac{d}{dr}\left(\frac{1}{\Delta}\frac{dR_{\ell m\omega}}{dr}\right) - V(r)R_{\ell m\omega} = T_{\ell m\omega}, \tag{2·1}$$

where the potential term $V(r)$ is given by

$$V(r) = -\frac{K^2 + 4i(r-M)K}{\Delta} + 8i\omega r + \lambda. \tag{2·2}$$

Here, $\Delta = r^2 - 2Mr + a^2 = (r - r_+)(r - r_-)$ with $r_\pm = M \pm \sqrt{M^2 - a^2}$, $K = (r^2 + a^2)\omega - ma$ and λ is the eigenvalue of the angular Teukolsky equation.

In the MST method, the homogeneous solutions of the Teukolsky equation are expressed in terms of two kinds of series of special functions.[23),27)] One consists of series of hypergeometric functions, and the other consists of series of Coulomb wave functions. The former is convergent at the horizon and the latter at infinity. We match the two kinds of solutions in the overlapping region of convergence. We thereby obtain analytical expressions of the asymptotic amplitudes of the solution. (See Ref. 25) for a more recent review.)

First, we present a solution consisting of a series of hypergeometric functions. For the incoming solution $R^{\rm in}_{lm\omega}$, we define $p_{\rm in}$ by

$$R^{\rm in}_{lm\omega} = e^{i\epsilon\kappa x}(-x)^{-s-i(\epsilon+\tau)/2}(1-x)^{i(\epsilon-\tau)/2}p_{\rm in}(x). \tag{2·3}$$

The function $p_{\rm in}$ is expressed in a series of hypergeometric functions as

$$p_{\rm in}(x) = \sum_{n=-\infty}^{\infty} a_n F(n+\nu+1-i\tau, -n-\nu-i\tau; 1-s-i\epsilon-i\tau; x), \tag{2·4}$$

where $x = \omega(r_+ - r)/\epsilon\kappa$, $\epsilon = 2M\omega, \kappa = \sqrt{1-q^2}, q = a/M, \tau = (\epsilon - mq)/\kappa$ and $F(\alpha, \beta; \gamma; x)$ is the hypergeometric function.

This expression can be rewritten, using the analytic properties of hypergeometric functions, into the form of a series expansion with better convergence properties for large $|x|$ as

$$R^{\rm in}_{lm\omega} = R^{\nu}_0 + R^{-\nu-1}_0, \tag{2·5}$$

where

$$\begin{aligned} R^{\nu}_0 = {} & e^{i\epsilon\kappa x}(-x)^{-s-\frac{i}{2}(\epsilon+\tau)}(1-x)^{\frac{i}{2}(\epsilon+\tau)+\nu} \\ & \times \sum_{n=-\infty}^{\infty} f^{\nu}_n \frac{\Gamma(1-s-i\epsilon-i\tau)\Gamma(2n+2\nu+1)}{\Gamma(n+\nu+1-i\tau)\Gamma(n+\nu+1-s-i\epsilon)} \\ & \times (1-x)^n F\left(-n-\nu-i\tau, -n-\nu-s-i\epsilon; -2n-2\nu; \frac{1}{1-x}\right). \end{aligned} \tag{2·6}$$

Next, we present a solution in the form of series of Coulomb wave functions. Let us denote a Teukolsky function by $R_{\rm C}$. We define the function $f_\nu(z)$ through the relation

$$R_{\rm C} = z^{-1-s}\left(1 - \frac{\epsilon\kappa}{z}\right)^{-s-i(\epsilon+\tau)/2} f_\nu(z). \tag{2·7}$$

The function $f_\nu(z)$ is expressed in a series of Coulomb wave functions as

$$f_\nu(z) = \sum_{n=-\infty}^{\infty} (-i)^n \frac{(\nu+1+s-i\epsilon)_n}{(\nu+1-s+i\epsilon)_n} a_n F_{n+\nu}(-is-\epsilon, z), \tag{2·8}$$

where $z = \omega(r - r_-)$, $(a)_n = \Gamma(a+n)/\Gamma(a)$ and $F_N(\eta, z)$ is a Coulomb wave function defined by

$$F_N(\eta, z) = e^{-iz}2^N z^{N+1}\frac{\Gamma(N+1-i\eta)}{\Gamma(2N+2)}\Phi(N+1-i\eta, 2N+2; 2iz). \tag{2·9}$$

Here $\Phi(\alpha,\beta;z)$ is the confluent hypergeometric function, which is regular at $z=0$ (see §13 of Ref. 28)).

In this method, the expansion coefficients of the series of hypergeometric functions and the series of Coulomb wave functions $\{a_n\}$ exhibit the same recurrence relation. We find that the expansion coefficients a_n satisfy the three-term recurrence relation

$$\alpha_n^\nu a_{n+1} + \beta_n^\nu a_n + \gamma_n^\nu a_{n-1} = 0, \tag{2·10}$$

where

$$\alpha_n^\nu = \frac{i\epsilon\kappa(n+\nu+1+s+i\epsilon)(n+\nu+1+s-i\epsilon)(n+\nu+1+i\tau)}{(n+\nu+1)(2n+2\nu+3)},$$

$$\beta_n^\nu = -\lambda - s(s+1) + (n+\nu)(n+\nu+1) + \epsilon^2 + \epsilon(\epsilon-mq) + \frac{\epsilon(\epsilon-mq)(s^2+\epsilon^2)}{(n+\nu)(n+\nu+1)},$$

$$\gamma_n^\nu = -\frac{i\epsilon\kappa(n+\nu-s+i\epsilon)(n+\nu-s-i\epsilon)(n+\nu-i\tau)}{(n+\nu)(2n+2\nu-1)}.$$

We note that the parameter ν introduced in the above formulas does not exist in the Teukolsky equation. This parameter is introduced so that both series converge and actually represent a solution of the Teukolsky equation. We next introduce the following quantities:

$$R_n \equiv \frac{a_n}{a_{n-1}}, \quad L_n \equiv \frac{a_n}{a_{n+1}}. \tag{2·11}$$

We can express R_n and L_n in terms of continued fractions as

$$\begin{aligned} R_n &= -\frac{\gamma_n^\nu}{\beta_n^\nu + \alpha_n^\nu R_{n+1}} \\ &= -\frac{\gamma_n^\nu}{\beta_n^\nu -}\,\frac{\alpha_n^\nu\gamma_{n+1}^\nu}{\beta_{n+1}^\nu -}\,\frac{\alpha_{n+1}^\nu\gamma_{n+2}^\nu}{\beta_{n+2}^\nu -}\cdots, \end{aligned} \tag{2·12}$$

$$\begin{aligned} L_n &= -\frac{\alpha_n^\nu}{\beta_n^\nu + \gamma_n^\nu L_{n-1}} \\ &= -\frac{\alpha_n^\nu}{\beta_n^\nu -}\,\frac{\alpha_{n-1}^\nu\gamma_n^\nu}{\beta_{n-1}^\nu -}\,\frac{\alpha_{n-2}^\nu\gamma_{n-1}^\nu}{\beta_{n-2}^\nu -}\cdots. \end{aligned} \tag{2·13}$$

The expressions for R_n and L_n are valid if these continued fractions converge. It has been proved[29] that the continued fraction of the right-hand side of Eq. (2·12) converges if and only if the recurrence relations Eq. (2·10) possess a minimal solution as $n\to\infty$. A similar theorem can be proven regarding the converge as $n\to-\infty$ of the right-hand side of Eq. (2·13). Because the recurrence relation Eq. (2·10) possesses minimal solutions as $n\to\pm\infty$, the continued fractions on the right-hand sides of Eqs. (2·12) and (2·13) converge. Although minimal solutions in the limits $n\to\infty$ and $n\to-\infty$ do not coincide in general, we can match them by appropriately choosing ν. Suppose $\{f_n^\nu\}$ is a solution that is minimal for both $n\to\pm\infty$. It is proved[29] that the following relations are satisfied:

$$\tilde{R}_n \equiv \frac{f_n^\nu}{f_{n-1}^\nu} = -\frac{\gamma_n^\nu}{\beta_n^\nu -}\,\frac{\alpha_n^\nu\gamma_{n+1}^\nu}{\beta_{n+1}^\nu -}\,\frac{\alpha_{n+1}^\nu\gamma_{n+2}^\nu}{\beta_{n+2}^\nu -}\cdots, \tag{2·14}$$

$$\tilde{L}_n^\nu \equiv \frac{f_n^\nu}{f_{n+1}^\nu} = -\frac{\alpha_n^\nu}{\beta_n^\nu -}\,\frac{\alpha_{n-1}^\nu \gamma_n^\nu}{\beta_{n-1}^\nu -}\,\frac{\alpha_{n-2}^\nu \gamma_{n-1}^\nu}{\beta_{n-2}^\nu -}\cdots . \tag{2·15}$$

This implies the relation

$$\tilde{R}_n \tilde{L}_{n-1} = 1. \tag{2·16}$$

If we choose ν such that it satisfies the implicit equation for ν, Eq. (2·16), for a certain n, we can obtain a minimal solution $\{f_n^\nu\}$ that is valid over the entire range $-\infty < n < \infty$. For the minimal solution, f_n^ν, we have

$$\lim_{n\to\infty} n\frac{f_n^\nu}{f_{n-1}^\nu} = \frac{i\epsilon\kappa}{2}, \quad \lim_{n\to-\infty} n\frac{f_n^\nu}{f_{n+1}^\nu} = -\frac{i\epsilon\kappa}{2}. \tag{2·17}$$

The minimal solution is important for the convergence of the series Eqs. (2·4) and (2·8). It can be proved that if we use the minimal solution $\{f_n^\nu\}$ for the expansion coefficients $\{a_n\}$, the series of hypergeometric functions Eq. (2·4) converges for x in the range $-\infty < x \le 0$. (In fact, this is true for all complex values of x, except at $|x| = \infty$.) It has also been proved that if the expansion coefficients are given by the minimal solution, the series Eq. (2·8) converges for $z > \epsilon\kappa$ or, equivalently, $r > r_+$.

Instead of Eq. (2·16), we can use an equivalent but practically more convenient form of an equation that determines the value of ν. Dividing Eq. (2·10) by a_n, we find

$$\beta_n^\nu + \alpha_n^\nu \tilde{R}_{n+1} + \gamma_n^\nu \tilde{L}_{n-1} = 0, \tag{2·18}$$

where R_{n+1} and L_{n-1} are given by the continued fractions Eqs. (2·14) and (2·15) respectively.

2.2. *Matching and the asymptotic amplitudes*

Now, we match the two kinds of solutions, R_0^ν and $R_{\rm C}^\nu$. If we expand solutions in powers of $\tilde{x} = 1 - x \equiv z/(\epsilon\kappa)$, we see that both solutions behave like $\tilde{x}^\nu$ multiplied by a single valued function of $\tilde{x}$ for large $|\ \tilde{x}\ |$, as long as $\omega > 0$. Thus, if we assume $\omega > 0$, the analytic properties of R_0^ν and $R_{\rm C}^\nu$ are the same. That implies that these two solutions are identical up to a constant multiple. We set

$$R_0^\nu = K_\nu R_{\rm C}^\nu. \tag{2·19}$$

Then, by comparing each power of $\tilde{x}$ in the region where both solutions converge, i.e. $1 \ll |\ \tilde{x}\ | < \infty$, we find

$$\begin{aligned} K_\nu = {} & \frac{e^{i\epsilon\kappa}(2\epsilon\kappa)^{s-\nu-N}2^{-s}i^N \Gamma(1-s-i\epsilon-i\tau)\Gamma(N+2\nu+2)}{\Gamma(N+\nu+1-s+i\epsilon)\Gamma(N+\nu+1+i\tau)\Gamma(N+\nu+1+s+i\epsilon)} \\ & \times \left(\sum_{n=N}^{\infty}(-1)^n \frac{\Gamma(n+N+2\nu+1)}{(n-N)!}\frac{\Gamma(n+\nu+1+s+i\epsilon)\Gamma(n+\nu+1+i\tau)}{\Gamma(n+\nu+1-s-i\epsilon)\Gamma(n+\nu+1-i\tau)} f_n^\nu\right) \\ & \times \left(\sum_{n=-\infty}^{N} \frac{(-1)^n}{(N-n)!(N+2\nu+2)_n}\frac{(\nu+1+s-i\epsilon)_n}{(\nu+1-s+i\epsilon)_n} f_n^\nu\right)^{-1}, \end{aligned} \tag{2·20}$$

where N can be any integer, and the factor K_ν should be independent of the choice of N.

Now, we have an alternative expression for the ingoing-wave function $R^{\rm in}_{lm\omega}$,

$$R^{\rm in}_{lm\omega} = K_\nu R^\nu_{\rm C} + K_{-\nu-1} R^{-\nu-1}_{\rm C}, \tag{2·21}$$

which converges for $r > r_+$, including $r = \infty$. Combining Eq. (2·21) with Eq. (2·4), which converges everywhere except at $r = \infty$, we have a complete set of analytic solutions for the ingoing-wave function.

Now, we can obtain analytical expressions for the asymptotic amplitudes $B^{\rm trans}_{lm\omega}$, $B^{\rm inc}_{lm\omega}$ and $B^{\rm ref}_{lm\omega}$, of $R^{\rm in}_{lm\omega}$ defined in Eq. (A·8). Comparing $R^{\rm in}_{lm\omega}$ with Eq. (2·4) in the limit of $r \to r_+$ and Eq. (2·21) in the limit of $r \to \infty$, we find

$$\begin{aligned}
B^{\rm trans}_{lm\omega} &= \left(\frac{\epsilon\kappa}{\omega}\right)^{2s} e^{i\frac{\epsilon+\tau}{2}\ln\kappa} \sum_{n=-\infty}^{\infty} f^\nu_n, \\
B^{\rm inc}_{lm\omega} &= \omega^{-1}\left[K_\nu - ie^{-i\pi\nu}\frac{\sin\pi(\nu-s+i\epsilon)}{\sin\pi(\nu+s-i\epsilon)}K_{-\nu-1}\right] A^\nu_+ e^{-i\epsilon\ln\epsilon}, \\
B^{\rm ref}_{lm\omega} &= \omega^{-1-2s}[K_\nu + ie^{i\pi\nu}K_{-\nu-1}] A^\nu_- e^{i\epsilon\ln\epsilon},
\end{aligned} \tag{2·22}$$

where

$$\begin{aligned}
A^\nu_+ &= 2^{-1+s-i\epsilon} e^{-\frac{\pi\epsilon}{2}} e^{\frac{\pi}{2}i(\nu+1-s)} \frac{\Gamma(\nu+1-s+i\epsilon)}{\Gamma(\nu+1+s-i\epsilon)} \sum_{n=-\infty}^{+\infty} f^\nu_n, \\
A^\nu_- &= 2^{-1-s+i\epsilon} e^{-\frac{\pi\epsilon}{2}} e^{\frac{-\pi}{2}i(\nu+1+s)} \sum_{n=-\infty}^{+\infty} (-1)^n \frac{(\nu+1+s-i\epsilon)_n}{(\nu+1-s+i\epsilon)_n} f^\nu_n.
\end{aligned} \tag{2·23}$$

We can also obtain an analytical expression for $R^{\rm up}_{lm\omega}$ by transforming $R_{\rm C}$. We note that an analytical property of the confluent hypergeometric function,

$$\Phi(\alpha,\gamma,x) = \frac{\Gamma(\gamma)}{\Gamma(\gamma-\alpha)} e^{i\alpha\pi\sigma}\Psi(\alpha,\gamma,x) + \frac{\Gamma(\gamma)}{\Gamma(\omega)} e^{i\pi(\alpha-\gamma)\sigma}\Psi(\gamma-\alpha,\gamma,-x). \tag{2·24}$$

Here $\sigma = {\rm sgn}[{\rm Im}(x)]$ and $\Psi(a,c,x)$ is the irregular confluent hypergeometric function. We then rewrite $R^\nu_{\rm C}$ as

$$R^\nu_{\rm C} = R^\nu_+ + R^\nu_-, \tag{2·25}$$

where

$$\begin{aligned}
R^\nu_+ &= 2^\nu e^{-\pi\epsilon} e^{i\pi(\nu+1-s)} \frac{\Gamma(\nu+1-s+i\epsilon)}{\Gamma(\nu+1+s-i\epsilon)} e^{-iz} z^{\nu+i(\epsilon+\tau)/2} (z-\epsilon\kappa)^{-s-i(\epsilon+\tau)/2} \\
&\quad \times \sum_{n=-\infty}^{\infty} i^n f^\nu_n (2z)^n \Psi(n+\nu+1-s+i\epsilon, 2n+2\nu+2; 2iz),
\end{aligned} \tag{2·26}$$

$$\begin{aligned}
R^\nu_- &= 2^\nu e^{-\pi\epsilon} e^{-i\pi(\nu+1+s)} e^{iz} z^{\nu+i(\epsilon+\tau)/2} (z-\epsilon\kappa)^{-s-i(\epsilon+\tau)/2} \sum_{n=-\infty}^{\infty} i^n \\
&\quad \times \frac{(\nu+1+s-i\epsilon)_n}{(\nu+1-s+i\epsilon)_n} f^\nu_n (2z)^n \Psi(n+\nu+1+s-i\epsilon, 2n+2\nu+2; -2iz).
\end{aligned} \tag{2·27}$$

For large $\mid x \mid$, $\Psi(\alpha, \gamma, x)$ behaves as

$$\Psi(\alpha, \beta, x) \to x^{-\alpha} \text{ as } \mid x \mid \to \infty. \tag{2·28}$$

We therefore have

$$\begin{aligned} R_+^\nu &= A_+^\nu z^{-1} e^{-i(z+\epsilon \ln z)}, \\ R_-^\nu &= A_-^\nu z^{-1-2s} e^{i(z+\epsilon \ln z)}. \end{aligned} \tag{2·29}$$

We can see that the functions R_+^ν and R_-^ν are ingoing-wave and outgoing-wave solutions at infinity, respectively. In particular, we have the upgoing solution expressed in terms of Coulomb wave functions as

$$R_{lm\omega}^{\text{up}} = R_-^\nu. \tag{2·30}$$

Now, we can obtain an analytical expression of the asymptotic amplitude, $C_{lm\omega}^{\text{trans}}$, of $R_{lm\omega}^{\text{up}}$ defined in Eq. (A·9). We find

$$C_{lm\omega}^{\text{trans}} = \omega^{-1-2s} e^{i\epsilon \ln \epsilon} A_-^\nu. \tag{2·31}$$

§3. Numerical methods

In order to compute the homogeneous solutions of the Teukolsky equation, we first compute the eigenvalue λ of the spin weighted spheroidal harmonics. This is discussed in Appendix B. In this section, we discuss a numerical method to compute the homogeneous solution of the radial part of the Teukolsky equation, assuming λ is given. The eigenvalue λ can be computed similar in to ν. Although the MST formalism was developed for arbitrary values of the spin s, in the rest of paper we consider only the case $s = -2$, because this is important to evaluate gravitational waves.

3.1. *Continued fractions*

Because the computation of continued fractions is very important in our numerical method, we first review *Steed's algorithm* to compute continued fractions.[30] Let us define a continued fraction by

$$h_n \equiv \frac{A_n}{B_n} = b_0 + \frac{a_1}{b_1+}\frac{a_2}{b_2+}\frac{a_3}{b_3+}\cdots\frac{a_n}{b_n}. \tag{3·1}$$

It can be shown that A_n and B_n satisfy the recurrence relations

$$\begin{pmatrix} A_n \\ B_n \end{pmatrix} = \begin{pmatrix} A_{n-1} & A_{n-2} \\ B_{n-1} & B_{n-2} \end{pmatrix} \begin{pmatrix} b_n \\ a_n \end{pmatrix}, \quad \begin{pmatrix} A_0 & A_{-1} \\ B_0 & B_{-1} \end{pmatrix} = \begin{pmatrix} b_0 & 1 \\ 1 & 0 \end{pmatrix}. \tag{3·2}$$

Here, we introduce the quantity $D_n = B_{n-1}/B_n$. Then, the above recurrence relation of B_n is identical to

$$D_n = \frac{1}{b_n + a_n D_{n-1}}. \tag{3·3}$$

We can rewrite the right-hand side of Eq. (3·1) in terms of D_n as

$$\begin{aligned} h_n = \frac{A_n}{B_n} &= \frac{b_n A_{n-1} + a_n A_{n-2}}{b_n B_{n-1} + a_n B_{n-2}}, \\ &= \frac{b_n (A_{n-1}/B_{n-1}) + a_n (A_{n-2}B_{n-2}/B_{n-2}B_{n-1})}{b_n + a_n (B_{n-2}/B_{n-1})}, \\ &= (h_{n-1} b_n + h_{n-2} D_{n-1} a_n) D_n. \end{aligned} \tag{3·4}$$

Furthermore, from Eq. (3·3), we have the relation $a_n D_{n-1} D_n = 1 - b_n D_n$, which then yields the difference between h_n and h_{n-1},

$$\begin{aligned} \Delta h_n &\equiv h_n - h_{n-1}, \\ &= (b_n D_n - 1)(h_{n-1} - h_{n-2}), \\ &= (b_n D_n - 1) \Delta h_{n-1}. \end{aligned} \tag{3·5}$$

Steed's algorithm is summarized as follows. We first set $h_0 = b_0$, $D_1 = 1/b_1$, $\Delta h_1 = a_1/b_1$ and $h_1 = h_0 + \Delta h_1$. We then compute h_n beginning with $n = 2$ until $| \Delta h_n / h_n |$ is smaller than the required accuracy.

3.2. *Determination of the renormalized angular momentum ν*

The parameter ν is determined as a solution of Eq. (2·18). In particular, we set $n = 0$ and obtain

$$g(\nu) \equiv \beta_0^\nu + \alpha_0^\nu \tilde{R}_1 + \gamma_0^\nu \tilde{L}_{-1} = 0, \tag{3·6}$$

where $\tilde{R}_1$ and $\tilde{L}_{-1}$ are expressed by the continued fractions Eqs. (2·14) and (2·15), respectively.

In order to search for a root of the implicit equation $g(\nu) = 0$, we can use various numerical techniques. Among them, we adopt *Brent's algorithm* (e.g. Ref. 31)). In

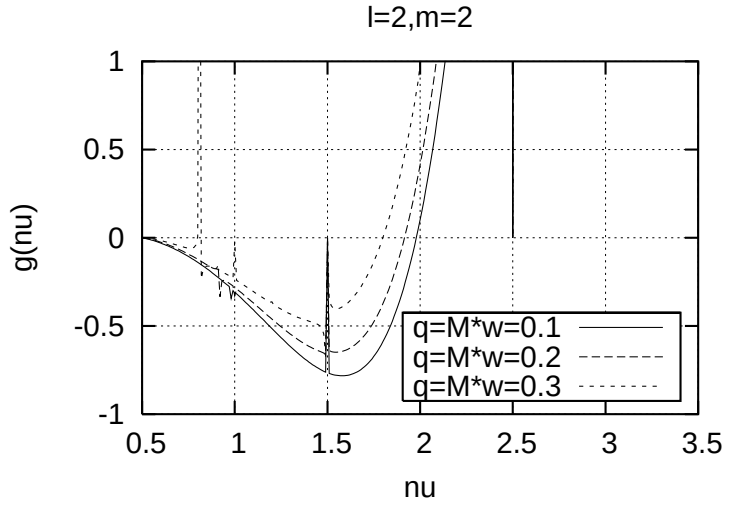

Fig. 1. $g(\nu)$ for $\ell = 2, m = 2$.

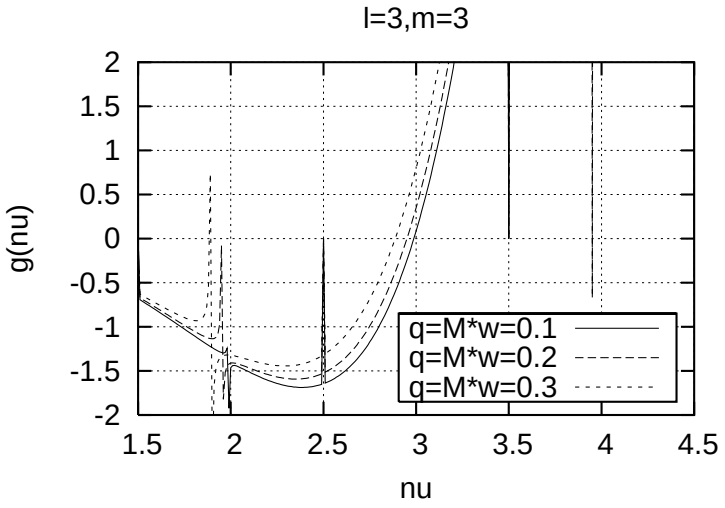

Fig. 2. $g(\nu)$ for $\ell = 3, m = 3$.

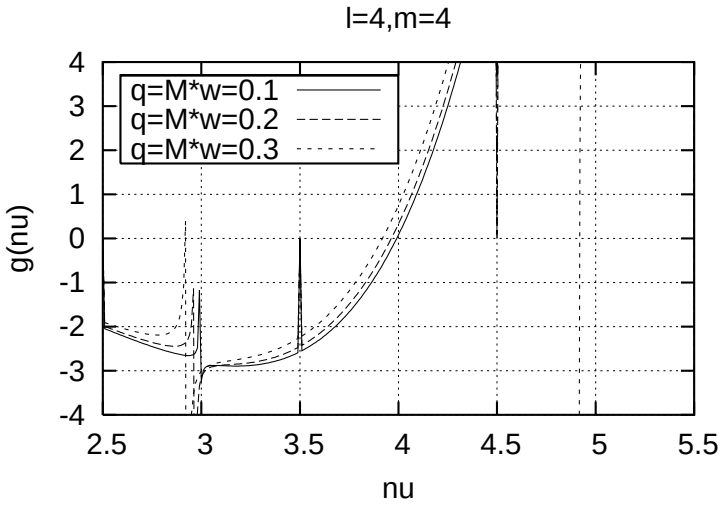

Fig. 3. $g(\nu)$ for $\ell = 4, m = 4$.

order to search for a root of implicit equations, we need an initial value of the search which is not very far away from the root of the equation. In the case that $M\omega$ is small, we can use an analytic expression of ν as the initial value. Among the infinite number of roots, there is an analytic expression of ν in the form of a series of $\epsilon \equiv 2M\omega$ given by

$$\nu = \ell + \frac{1}{2\ell+1}\left[-2 - \frac{s^2}{\ell(\ell+1)} + \frac{[(\ell+1)^2 - s^2]^2}{(2\ell+1)(2\ell+2)(2\ell+3)} - \frac{(\ell^2-s^2)^2}{(2\ell-1)2\ell(2\ell+1)}\right]\epsilon^2 + O(\epsilon^3). \tag{3·7}$$

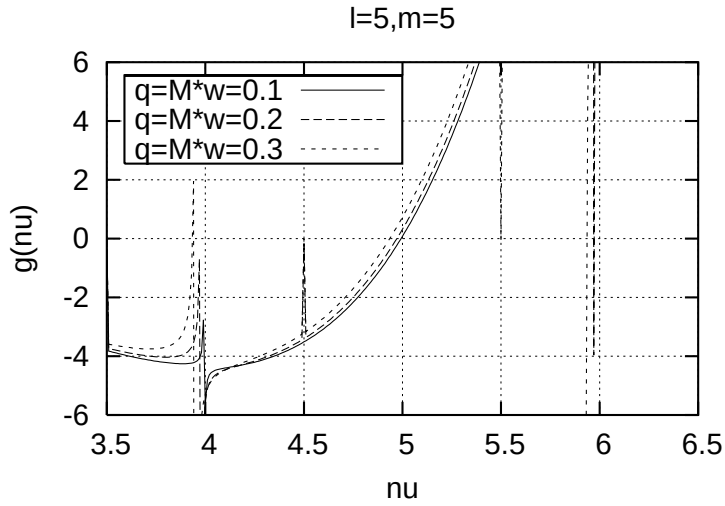

Fig. 4. $g(\nu)$ for $\ell = 5, m = 5$.

When $M\omega$ is not very large (less than ~ 0.36 in the case $q = 0$), this expression is useful as an initial value for the root search algorithm. Note that the analytic expression for ν truncated at $O(\epsilon^2)$ is always slightly less than ℓ. Thus, in practice, it is sufficient to search for a root in the range $\ell - 1/2 < \nu < \ell$. We can see in Figs. 1–4 that the function $g(\nu)$ is smooth in this range. Although numerically we find poles at half integer values of ν, it is not difficult to find a root in this region. In fact, we can find a root as long as $M\omega \lesssim 0.36$ in the case $\ell = m = 2$ and $q = 0$.

However, the situation is different when $M\omega$ becomes larger. In this case, ν approaches $\ell - 1/2$, and beyond a certain value of $M\omega$, it becomes impossible to find roots ν. The maximum values of $M\omega$ for which real ν can be found in the region $\ell - 1/2 < \nu < \ell$ are listed in Table I. The maximum values depend on ℓ, m and q. This maximum value of $M\omega$ increases with ℓ. The maximum value is larger for $q > 0$ than for $q < 0$. The behavior of ν beyond $M\omega$ in Table I depends on ℓ and m. In some cases, we can find ν as a real value. However, in other cases, there is no root of Eq. (3·6) for any real value of ν.

We note that we have attempted to find a complex root ν. Our preliminary investigation suggests that there is such a root in the complex value of ν when we cannot find a real root. However, more work is needed to confirm this, and we leave this as a future project. In the rest of this paper, we concentrate on the case of real ν and the region of ϵ in which we can find such a root. The values of ν for various values of $M\omega = \epsilon/2$, ℓ, and q are plotted in Fig. 5.

Note that there are some roots at integer and half integer values of ν that are independent of ℓ, m, q, and ω. Although they are solutions of $g(\nu) = 0$, they do not connect the two minimal solutions in the limits $n \to \pm\infty$.

When ν is a root of Eq. (3·6), the quantities $\nu + k$ ($k = \pm 1, \pm 2, \cdots$) are also roots of Eq. (3·6), since ν only appears as $\nu + n$ in the continued fractions of Eq. (3·6). This fact can be checked numerically for $k = \pm 1$. However, as we can see in Figs. 1–4,

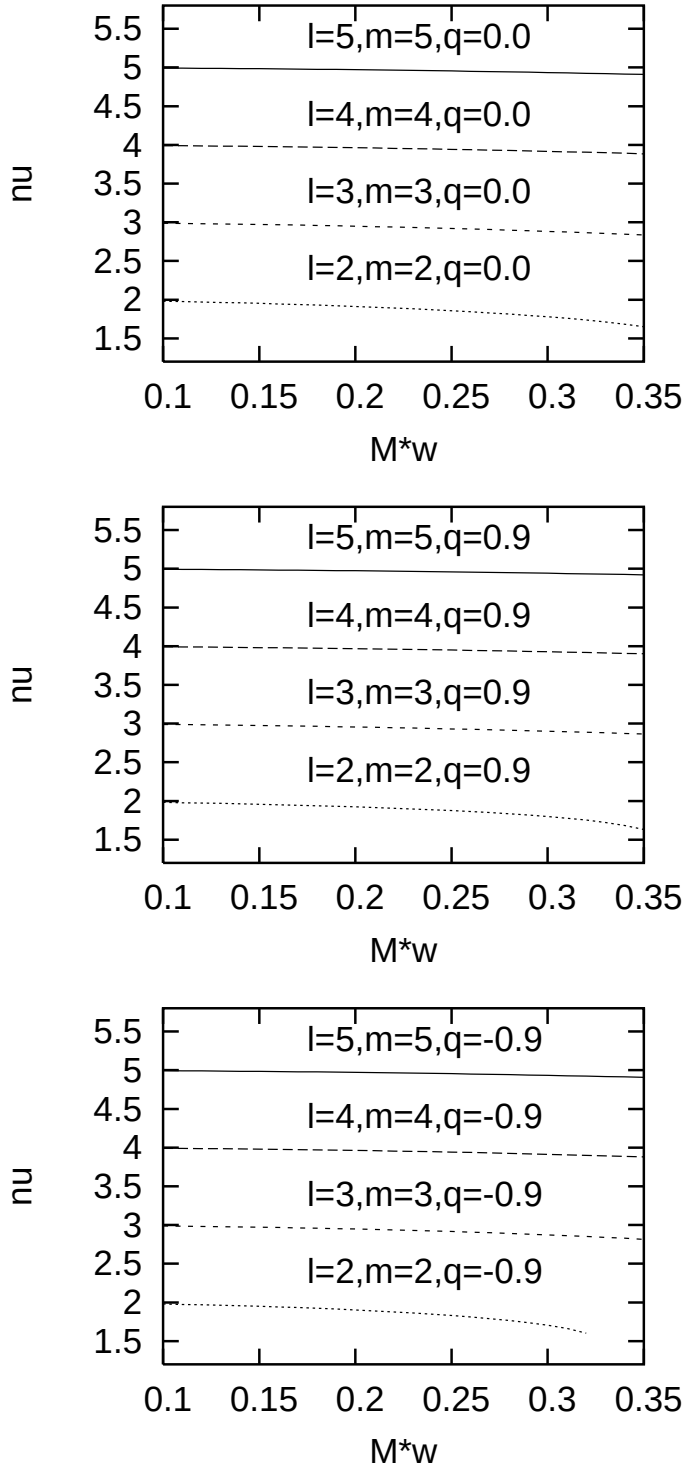

Fig. 5. ν as a function of $M\omega$ for $\ell = m = 2$ to $\ell = m = 5$ for $q = 0$, 0.9 and -0.9.

Table I. Maximum values of $M\omega$ for which real ν is found.

ℓ	m	$q=0.9$	$q=0$	$q=-0.9$	ℓ	m	$q=0.9$	$q=0$	$q=-0.9$
2	2	0.39	0.36	0.32	8	8	1.08	1.00	0.92
2	1	0.44	0.36	0.34	8	7	1.07	1.00	0.93
2	0	0.38	0.36	0.38	8	6	1.06	1.00	0.94
3	3	0.58	0.53	0.45	8	5	1.05	1.00	0.95
3	2	0.61	0.53	0.48	8	4	1.04	1.00	0.96
3	1	0.59	0.53	0.51	8	3	1.03	1.00	0.97
3	0	0.55	0.53	0.55	8	2	1.02	1.00	0.98
4	4	0.73	0.66	0.57	8	1	1.01	1.00	0.99
4	3	0.73	0.66	0.60	8	0	1.00	1.00	1.00
4	2	0.72	0.66	0.63	9	9	1.14	1.06	0.99
4	1	0.70	0.66	0.65	9	8	1.13	1.06	1.00
4	0	0.68	0.66	0.68	9	7	1.12	1.06	1.00
5	5	0.84	0.77	0.68	9	6	1.12	1.06	1.01
5	4	0.83	0.77	0.70	9	5	1.11	1.06	1.02
5	3	0.82	0.77	0.72	9	4	1.10	1.06	1.03
5	2	0.80	0.77	0.74	9	3	1.09	1.06	1.04
5	1	0.79	0.77	0.76	9	2	1.08	1.06	1.05
5	0	0.77	0.77	0.77	9	1	1.07	1.06	1.06
6	6	0.93	0.85	0.77	9	0	1.06	1.06	1.06
6	5	0.92	0.85	0.79	10	10	1.20	1.12	1.05
6	4	0.91	0.85	0.80	10	9	1.19	1.12	1.05
6	3	0.89	0.85	0.82	10	8	1.19	1.12	1.06
6	2	0.88	0.85	0.83	10	7	1.18	1.12	1.07
6	1	0.87	0.85	0.84	10	6	1.17	1.12	1.08
6	0	0.86	0.85	0.86	10	5	1.16	1.12	1.09
7	7	1.01	0.93	0.85	10	4	1.16	1.12	1.09
7	6	1.00	0.93	0.86	10	3	1.15	1.12	1.10
7	5	0.99	0.93	0.88	10	2	1.14	1.12	1.11
7	4	0.98	0.93	0.89	10	1	1.13	1.12	1.12
7	3	0.96	0.93	0.90	10	0	1.12	1.12	1.12
7	2	0.95	0.93	0.91					
7	1	0.94	0.93	0.92					
7	0	0.93	0.93	0.93					

the function $g(\nu)$ around the roots $\nu \pm 1$ is a very steep function. When $|k|$ is larger than 2, the slope of $g(\nu)$ becomes much steeper, and it becomes difficult to find the root $\nu + k$.

3.3. *Expansion coefficients*

Once we have ν, it is straightforward to evaluate the expansion coefficients using the three-term recurrence relations Eq. (2·10). As discussed in §2, the expansion coefficients $\{a_n\}$ must be the minimal solution $\{f_n\}$. It is well known that the minimal solution cannot be computed numerically with forward recursion of the three-term recurrence relations from $n = 0$ to $\pm\infty$. This is because a small numerical errors in the minimal solution f_n contain dominant parts of the solution of the recurrence relation. For this reason, the numerical solution obtained using forward recursion will be dominated by errors after several recursions, since the dominant

Table II. ν for $M\omega = 0.1$.

ℓ	m	$q = -0.9$	$q = 0$	$q = 0.9$
2	2	1.9780030721	1.9793154547	1.9805149449
2	1	1.9787154140	1.9793154547	1.9799783120
2	0	1.9793759881	1.9793154547	1.9793759881
2	−1	1.9799783120	1.9793154547	1.9787154140
2	−2	1.9805149449	1.9793154547	1.9780030721
3	3	2.9871135866	2.9875539197	2.9879712028
3	2	2.9872683427	2.9875539197	2.9878392372
3	1	2.9874180082	2.9875539197	2.9877032005
3	0	2.9875628720	2.9875539197	2.9875628720
3	−1	2.9877032005	2.9875539197	2.9874180082
3	−2	2.9878392372	2.9875539197	2.9872683427
3	−3	2.9879712028	2.9875539197	2.9871135866
4	4	3.9906679155	3.9909066870	3.9911355283
4	3	3.9907299644	3.9909066870	3.9910804817
4	2	3.9907909277	3.9909066870	3.9910245146
4	1	3.9908508359	3.9909066870	3.9909676019
4	0	3.9909097180	3.9909066870	3.9909097180
4	−1	3.9909676019	3.9909066870	3.9908508359
4	−2	3.9910245146	3.9909066870	3.9907909277
4	−3	3.9910804817	3.9909066870	3.9907299644
4	−4	3.9911355283	3.9909066870	3.9906679155
5	5	4.9926264974	4.9927797435	4.9929276871
5	4	4.9926581101	4.9927797435	4.9928989965
5	3	4.9926893758	4.9927797435	4.9928700024
5	2	4.9927203003	4.9927797435	4.9928406998
5	1	4.9927508893	4.9927797435	4.9928110837
5	0	4.9927811486	4.9927797435	4.9927811486
5	−1	4.9928110837	4.9927797435	4.9927508893
5	−2	4.9928406998	4.9927797435	4.9927203003
5	−3	4.9928700024	4.9927797435	4.9926893758
5	−4	4.9928989965	4.9927797435	4.9926581101
5	−5	4.9929276871	4.9927797435	4.9926264974
6	6	5.9938843772	5.9939919474	5.9940963285
6	5	5.9939027772	5.9939919474	5.9940793756
6	4	5.9939210379	5.9939919474	5.9940622984
6	3	5.9939391609	5.9939919474	5.9940450957
6	2	5.9939571478	5.9939919474	5.9940277660
6	1	5.9939750003	5.9939919474	5.9940103079
6	0	5.9939927198	5.9939919474	5.9939927198
6	−1	5.9940103079	5.9939919474	5.9939750003
6	−2	5.9940277660	5.9939919474	5.9939571478
6	−3	5.9940450957	5.9939919474	5.9939391609
6	−4	5.9940622984	5.9939919474	5.9939210379
6	−5	5.9940793756	5.9939919474	5.9939027772
6	−6	5.9940963285	5.9939919474	5.9938843772

solutions grow very rapidly.

In such a situation, we can use the continued fractions given in Eqs. (2·14) and (2·15) to evaluate the minimal solution. First, we set the initial value of f_n as $f_0 = 1$. We evaluate f_1 from f_1/f_0, which is evaluated by the continued fraction, the right-hand side of Eq. (2·14) with $n = 1$. We then obtain f_1 as $f_1 = \tilde{R}_1 f_0$. In the same way, we can evaluate f_n ($n > 1$) from f_{n-1} and $\tilde{R}_n$ recursively. For $n < 0$, we use the same algorithm and evaluate f_n from f_{n+1} and $\tilde{L}_n$.

3.4. *Homogeneous solutions*

Given the eigenvalue of the spin weighted spheroidal harmonics λ, the renormalized angular momentum ν, and the expansion coefficients f_n, it is straightforward to compute the asymptotic amplitude of the homogeneous solutions, Eqs. (2·22) and (2·31). It is also straightforward to compute the homogeneous functions using Eq. (2·3) or Eq. (2·30). We found that the convergence of the series of hypergeometric functions or Coulomb wave functions and that of the formulas for the asymptotic amplitude are very rapid. This is because the expansion coefficients $\{f_n^\nu\}$, which constitute a minimal solution of the three-term recurrence relation, decrease very rapidly as $|n|$ becomes large, as can be seen from Eq. (2·17). For example, we only need to carry out the summation in Eq. (2·4) from $n = 0$ to $n \sim \pm 20$ to have an accuracy 10^{-16} in the case $\epsilon < 0.4$.

The hypergeometric function $F(\alpha, \beta; \gamma, x)$ is computed using the transformation formula

$$\begin{aligned} F(\alpha,\beta;\gamma,x) = (1-x)^{-\alpha}\frac{\Gamma(\gamma)\Gamma(\beta-\alpha)}{\Gamma(\beta)\Gamma(\gamma-\alpha)}F\left(\alpha,\gamma-\beta;\alpha-\beta+1;\frac{1}{1-x}\right) \\ +(1-x)^{-\beta}\frac{\Gamma(\gamma)\Gamma(\alpha-\beta)}{\Gamma(\alpha)\Gamma(\gamma-\beta)}F\left(\beta,\gamma-\alpha;\beta-\alpha+1;\frac{1}{1-x}\right), \quad (3\cdot8) \end{aligned}$$

and using the Gauss hypergeometric series for the hypergeometric functions on the right-hand side of Eq. (3·8). For the gamma function, we use the routines available on the world wide web.[32)]

3.5. *Gravitational wave luminosity*

In order to check the accuracy of our numerical code, we calculated the gravitational wave flux from a point particle in circular orbits on the equatorial plane around a Kerr black hole. The formula for the luminosity is given in Appendix A.

Our computations presented here were done using a double precision code. In Tables III–VI, we list the luminosities for $r_0 = 6$, 10, 100 and 1000 from $\ell = 2$ to 6 and for $q = 0$ and $q = \pm 0.9$. We also list the total luminosity for various values q and r_0 in Table VII.

We compared these results with those of Tagoshi and Nakamura[22)] in the Schwarzschild case $q = 0$. The results are given in Table VIII for cases $r_0 = 10M$. We find that our results agree with them with relative error 10^{-14} – 10^{-15}. Because the estimated accuracy of Ref. 22) is more than 20 significant figures, we estimate that the accuracy of our code is about 13–14 significant figures. We also compare

Table III. The gravitational wave luminosity for $r_0 = 6M$.

ℓ	$\mid m \mid$	$q = -0.9$	$q = 0$	$q = 0.9$
2	2	$1.4672643416 \times 10^{-3}$	$7.3475638881 \times 10^{-4}$	$4.6183912921 \times 10^{-4}$
2	1	$2.4135187915 \times 10^{-5}$	$5.0413451839 \times 10^{-6}$	$6.6947435866 \times 10^{-7}$
3	3	$3.4798321412 \times 10^{-4}$	$1.4534938751 \times 10^{-4}$	$8.0343009373 \times 10^{-5}$
3	2	$1.0938697387 \times 10^{-5}$	$2.0567575315 \times 10^{-6}$	$2.9212522769 \times 10^{-7}$
3	1	$4.3891293595 \times 10^{-8}$	$1.1384270937 \times 10^{-8}$	$4.3010746650 \times 10^{-9}$
4	4	$1.0477344711 \times 10^{-4}$	$3.5849943696 \times 10^{-5}$	$1.7293785265 \times 10^{-5}$
4	3	$3.9195590828 \times 10^{-6}$	$6.2995356560 \times 10^{-7}$	$8.6369900044 \times 10^{-8}$
4	2	$7.5231697792 \times 10^{-8}$	$1.7547382460 \times 10^{-8}$	$6.1994559709 \times 10^{-9}$
4	1	$4.5312182607 \times 10^{-11}$	$7.0534448975 \times 10^{-12}$	$9.3343722027 \times 10^{-13}$
5	5	$3.4447343626 \times 10^{-5}$	$9.5758155537 \times 10^{-6}$	$4.0148159555 \times 10^{-6}$
5	4	$1.3473368296 \times 10^{-6}$	$1.8048918361 \times 10^{-7}$	$2.2863071277 \times 10^{-8}$
5	3	$5.0155535469 \times 10^{-8}$	$1.0218507481 \times 10^{-8}$	$3.3101913526 \times 10^{-9}$
5	2	$2.3873981915 \times 10^{-10}$	$3.1974516361 \times 10^{-11}$	$3.9575575812 \times 10^{-12}$
5	1	$4.8597838388 \times 10^{-14}$	$9.3414524994 \times 10^{-15}$	$2.8261985682 \times 10^{-15}$
6	6	$1.1820336377 \times 10^{-5}$	$2.6570852921 \times 10^{-6}$	$9.6579842085 \times 10^{-7}$
6	5	$4.5987487190 \times 10^{-7}$	$5.0650467610 \times 10^{-8}$	$5.7941986759 \times 10^{-9}$
6	4	$2.5069319096 \times 10^{-8}$	$4.3708099159 \times 10^{-9}$	$1.2798607028 \times 10^{-9}$
6	3	$2.7050690849 \times 10^{-10}$	$3.0671520252 \times 10^{-11}$	$3.4745761467 \times 10^{-12}$
6	2	$8.1558279125 \times 10^{-13}$	$1.3490851660 \times 10^{-13}$	$3.6798960699 \times 10^{-14}$
6	1	$2.8413832649 \times 10^{-17}$	$3.3772691941 \times 10^{-18}$	$3.9283478383 \times 10^{-19}$

our results with those given by Kennefick*) in the Kerr case $q \neq 0$. The results are given in Table IX for cases $r_0 = 3M$ and $q = 0.998$. We find that our results agree with them with relative error 10^{-6} – 10^{-7}. This is consistent with the estimated accuracy in his works. Although we do not have a quantitative estimate of the accuracy for the luminosity in the Kerr case, because ν is computed with accuracy in the Schwarzschild case, we expect that the accuracy of our results is also about 13–14 significant figures in the Kerr case.

§4. Summary and discussion

In this paper, we described numerical methods to compute the homogeneous solutions of the Teukolsky equation. We used the MST formalism, in which the homogeneous solutions of the Teukolsky equation are expressed in terms of series of hypergeometric functions and Coulomb wave functions. We found that the renormalized angular momentum ν can be found only for a limited values of $M\omega$. When $M\omega$ becomes large, ν approaches $\ell - 1/2$, and over a certain range of values of $M\omega$, which depends on ℓ, m and q, we could not find real ν. Our preliminary investigations suggest that ν becomes complex when $M\omega$ becomes sufficiently large. However, because further investigation is needed to confirm this, we continue to work on this point.

In the region of $M\omega$ in which we can find real ν, we found that the convergence of

*) This data was calculated by D. Kennefick based on his previous work,[16] and was kindly provided for us.

Table IV. The gravitational wave luminosity for $r_0 = 10M$.

ℓ	$\mid m \mid$	$q = -0.9$	$q = 0$	$q = 0.9$
2	2	$6.8120258138 \times 10^{-5}$	$5.3687954791 \times 10^{-5}$	$4.4546001102 \times 10^{-5}$
2	1	$5.0656468066 \times 10^{-7}$	$1.9316093512 \times 10^{-7}$	$5.2735787002 \times 10^{-8}$
3	3	$8.7890229491 \times 10^{-6}$	$6.4260827562 \times 10^{-6}$	$5.0413559470 \times 10^{-6}$
3	2	$1.2628541265 \times 10^{-7}$	$4.7959164616 \times 10^{-8}$	$1.4271936289 \times 10^{-8}$
3	1	$9.7967935639 \times 10^{-10}$	$5.7148989126 \times 10^{-10}$	$3.7294384569 \times 10^{-10}$
4	4	$1.4106496214 \times 10^{-6}$	$9.5396003949 \times 10^{-7}$	$7.0641315437 \times 10^{-7}$
4	3	$2.4037498342 \times 10^{-8}$	$8.7787575252 \times 10^{-9}$	$2.6507201263 \times 10^{-9}$
4	2	$9.3303939387 \times 10^{-10}$	$5.2622453090 \times 10^{-10}$	$3.3420025690 \times 10^{-10}$
4	1	$4.1524457529 \times 10^{-13}$	$1.4575856423 \times 10^{-13}$	$4.2218942492 \times 10^{-14}$
5	5	$2.4401253104 \times 10^{-7}$	$1.5241547646 \times 10^{-7}$	$1.0642982525 \times 10^{-7}$
5	4	$4.3181478959 \times 10^{-9}$	$1.4921162749 \times 10^{-9}$	$4.4382292146 \times 10^{-10}$
5	3	$3.3947862663 \times 10^{-10}$	$1.8291013252 \times 10^{-10}$	$1.1221183734 \times 10^{-10}$
5	2	$1.1385202800 \times 10^{-12}$	$3.8193532372 \times 10^{-13}$	$1.0943525441 \times 10^{-13}$
5	1	$4.6491185735 \times 10^{-16}$	$2.3676371874 \times 10^{-16}$	$1.3782555714 \times 10^{-16}$
6	6	$4.3683996396 \times 10^{-8}$	$2.5182131568 \times 10^{-8}$	$1.6571971666 \times 10^{-8}$
6	5	$7.6349317589 \times 10^{-10}$	$2.4746386947 \times 10^{-10}$	$7.1425097921 \times 10^{-11}$
6	4	$9.1394784860 \times 10^{-11}$	$4.6633398847 \times 10^{-11}$	$2.7471342862 \times 10^{-11}$
6	3	$6.6822442144 \times 10^{-13}$	$2.1238827476 \times 10^{-13}$	$5.9371098714 \times 10^{-14}$
6	2	$4.0965704268 \times 10^{-15}$	$1.9763689535 \times 10^{-15}$	$1.1021357357 \times 10^{-15}$
6	1	$1.1358089132 \times 10^{-19}$	$3.5977953599 \times 10^{-20}$	$9.9623097231 \times 10^{-21}$

the series of hypergeometric functions or Coulomb wave functions is very rapid. This is because the expansion coefficients $\{f_n^\nu\}$, which constitute a minimal solution of the three-term recurrence relation, decrease very rapidly as $|n|$ becomes large. Thus, we concluded that the MST formalism is a powerful method to compute the homogeneous solutions numerically. By comparing the numerical data for the gravitational wave luminosity emitted to infinity in the case that a particle display circular orbits in the equatorial plane with the results of previous works, we estimated the accuracy of our code to be about 13–14 significant figures in the double precision computation. This accuracy will be sufficient as a Green function of the Teukolsky equation in the computation of the templates for the data analysis of LISA. Currently, the accuracy is limited not by the MST formalism itself but by the accuracy of the evaluation of the hypergeometric functions.

In the near future, we will investigate the question of whether complex ν exist in order to broaden the region of $M\omega$, in which this method can be applied. We also hope to improve the accuracy of the evaluation of the hypergeometric functions and Coulomb wave functions and to apply this method to the computation of gravitational waves from a compact star in the case of more generic orbits around a supermassive black hole.

Acknowledgements

We thank D. Kennefick for kindly providing us his numerical data of the gravitational wave luminosity computed with the code developed in his work.[16] We thank M. Sasaki for useful discussions and continuous encouragement. We also thank F.

Table V. The gravitational wave luminosity for $r_0 = 100M$.

ℓ	$\mid m \mid$	$q = -0.9$	$q = 0$	$q = 0.9$
2	2	$6.1883920768 \times 10^{-10}$	$6.1534957152 \times 10^{-10}$	$6.1208585286 \times 10^{-10}$
2	1	$2.2912106158 \times 10^{-13}$	$1.7672378807 \times 10^{-13}$	$1.3144823366 \times 10^{-13}$
3	3	$8.2148864045 \times 10^{-12}$	$8.1530505104 \times 10^{-12}$	$8.0957455570 \times 10^{-12}$
3	2	$6.2294067784 \times 10^{-15}$	$4.9252050773 \times 10^{-15}$	$3.7844616487 \times 10^{-15}$
3	1	$7.6794049338 \times 10^{-16}$	$7.5711224891 \times 10^{-16}$	$7.4713604631 \times 10^{-16}$
4	4	$1.3404252509 \times 10^{-13}$	$1.3278019616 \times 10^{-13}$	$1.3161763785 \times 10^{-13}$
4	3	$1.2347499275 \times 10^{-16}$	$9.8769443625 \times 10^{-17}$	$7.7063402323 \times 10^{-17}$
4	2	$7.6509385330 \times 10^{-17}$	$7.5369817847 \times 10^{-17}$	$7.4317624281 \times 10^{-17}$
4	1	$2.6875757595 \times 10^{-21}$	$2.1456137700 \times 10^{-21}$	$1.6707364028 \times 10^{-21}$
5	5	$2.3376726712 \times 10^{-15}$	$2.3112411600 \times 10^{-15}$	$2.2870144702 \times 10^{-15}$
5	4	$2.2627547216 \times 10^{-18}$	$1.8214609703 \times 10^{-18}$	$1.4332319114 \times 10^{-18}$
5	3	$2.8901658332 \times 10^{-18}$	$2.8441315803 \times 10^{-18}$	$2.8016548481 \times 10^{-18}$
5	2	$7.3789391681 \times 10^{-22}$	$5.9290982541 \times 10^{-22}$	$4.6565092272 \times 10^{-22}$
5	1	$4.6833027135 \times 10^{-24}$	$4.5980275148 \times 10^{-24}$	$4.5192415969 \times 10^{-24}$
6	6	$4.1958033380 \times 10^{-17}$	$4.1404427415 \times 10^{-17}$	$4.0898989226 \times 10^{-17}$
6	5	$4.0369200351 \times 10^{-20}$	$3.2613208135 \times 10^{-20}$	$2.5791601982 \times 10^{-20}$
6	4	$8.0084356788 \times 10^{-20}$	$7.8709992082 \times 10^{-20}$	$7.7444340187 \times 10^{-20}$
6	3	$4.3274432473 \times 10^{-23}$	$3.4903584660 \times 10^{-23}$	$2.7554781747 \times 10^{-23}$
6	2	$4.1046272249 \times 10^{-24}$	$4.0245352816 \times 10^{-24}$	$3.9505730568 \times 10^{-24}$
6	1	$1.0005467982 \times 10^{-29}$	$8.0635499224 \times 10^{-30}$	$6.3602915489 \times 10^{-30}$

Takahara for continuous encouragement. H. T. thanks K. S. Thorne for continuous encouragement and his hospitality while staying at California Institute of Technology, where a part of this work was done, as a Zaigai Kenkyuin of Monbukagaku-sho. This work was supported in part by Monbukagaku-sho Grant-in-Aid for Scientific Research (Nos. 14047214, 12640269 and 16540251).

Appendix A
—— *Teukolsky Formalism* ——

A.1. *Teukolsky equation*

In terms of the Boyer-Lindquist coordinates (t, r, θ, ϕ), the metric of a Kerr black hole is expressed as

$$\begin{aligned} ds^2 = &- \frac{\Delta}{\Sigma}(dt - a\sin^2\theta d\phi)^2 + \frac{\sin^2\theta}{\Sigma}\left[(r^2+a^2)d\phi - a\,dt\right]^2 \\ &+ \frac{\Sigma}{\Delta}dr^2 + \Sigma d\theta^2 \equiv g_{\alpha\beta}dx^\alpha dx^\beta. \end{aligned} \tag{A·1}$$

where $\Sigma = r^2 + a^2\cos^2\theta$ and $\Delta = r^2 - 2Mr + a^2$. In the Teukolsky formalism,[4] the gravitational perturbations of a Kerr black hole are described by the Newman-Penrose quantity $\psi_4 = -C_{\alpha\beta\gamma\delta}n^\alpha\overline{m}^\beta n^\gamma\overline{m}^\delta$, where $C_{\alpha\beta\gamma\delta}$ is the Weyl tensor and

$$\begin{aligned} n^\alpha &= \left[(r^2+a^2), -\Delta, 0, a\right]/(2\Sigma), \\ m^\alpha &= \left[ia\sin\theta, 0, 1, i/\sin\theta\right]/(\sqrt{2}(r + ia\sin\theta)), \\ \overline{m}^\alpha &= \left[-ia\sin\theta, 0, 1, -i/\sin\theta\right]/(\sqrt{2}(r - ia\sin\theta)). \end{aligned} \tag{A·2}$$

Table VI. The gravitational wave luminosity for $r_0 = 1000M$.

ℓ	$\mid m \mid$	$q = -0.9$	$q = 0$	$q = 0.9$
2	2	$6.3710447707 \times 10^{-15}$	$6.3699449938 \times 10^{-15}$	$6.3688661222 \times 10^{-15}$
2	1	$1.9312210104 \times 10^{-19}$	$1.7759713679 \times 10^{-19}$	$1.6272619997 \times 10^{-19}$
3	3	$8.6164205339 \times 10^{-18}$	$8.6144354096 \times 10^{-18}$	$8.6124927366 \times 10^{-18}$
3	2	$5.4522769983 \times 10^{-22}$	$5.0596103733 \times 10^{-22}$	$4.6817315382 \times 10^{-22}$
3	1	$7.8992896709 \times 10^{-22}$	$7.8958536669 \times 10^{-22}$	$7.8924917557 \times 10^{-22}$
4	4	$1.4308259101 \times 10^{-20}$	$1.4304135903 \times 10^{-20}$	$1.4300106837 \times 10^{-20}$
4	3	$1.1099463480 \times 10^{-24}$	$1.0346766311 \times 10^{-24}$	$9.6207662590 \times 10^{-25}$
4	2	$8.0054989997 \times 10^{-24}$	$8.0018141364 \times 10^{-24}$	$7.9982051838 \times 10^{-24}$
4	1	$2.4183146906 \times 10^{-29}$	$2.2541754488 \times 10^{-29}$	$2.0958722688 \times 10^{-29}$
5	5	$2.5377450811 \times 10^{-23}$	$2.5368671349 \times 10^{-23}$	$2.5360100929 \times 10^{-23}$
5	4	$2.0796404136 \times 10^{-27}$	$1.9438447940 \times 10^{-27}$	$1.8126926234 \times 10^{-27}$
5	3	$3.0770492071 \times 10^{-26}$	$3.0755338762 \times 10^{-26}$	$3.0740495814 \times 10^{-26}$
5	2	$6.7754641895 \times 10^{-31}$	$6.3326624808 \times 10^{-31}$	$5.9050352599 \times 10^{-31}$
5	1	$4.9684166900 \times 10^{-32}$	$4.9656062758 \times 10^{-32}$	$4.9628506310 \times 10^{-32}$
6	6	$4.6302492101 \times 10^{-26}$	$4.6283797773 \times 10^{-26}$	$4.6265561943 \times 10^{-26}$
6	5	$3.7846535394 \times 10^{-30}$	$3.5438278934 \times 10^{-30}$	$3.3110410807 \times 10^{-30}$
6	4	$8.6738999088 \times 10^{-29}$	$8.6692973914 \times 10^{-29}$	$8.6647902975 \times 10^{-29}$
6	3	$4.0483295654 \times 10^{-33}$	$3.7905188064 \times 10^{-33}$	$3.5413297645 \times 10^{-33}$
6	2	$4.4179556837 \times 10^{-33}$	$4.4152753953 \times 10^{-33}$	$4.4126466761 \times 10^{-33}$
6	1	$9.4073281205 \times 10^{-40}$	$8.8079986933 \times 10^{-40}$	$8.2287305560 \times 10^{-40}$

Table VII. The gravitational wave luminosity, up through $\ell = 6$, for various q and orbital radii r_0/M.

r_0/M	$q = -0.9$	$q = -0.6$	$q = -0.3$	$q = 0$	$q = 0.3$	$q = 0.6$	$q = 0.9$
6	2.0073×10^{-3}	1.5089×10^{-3}	1.1707×10^{-3}	9.3619×10^{-4}	7.7061×10^{-4}	6.5182×10^{-4}	5.6555×10^{-4}
8	2.9124×10^{-4}	2.5217×10^{-4}	2.2097×10^{-4}	1.9593×10^{-4}	1.7577×10^{-4}	1.5948×10^{-4}	1.4631×10^{-4}
10	7.9272×10^{-5}	7.2377×10^{-5}	6.6505×10^{-5}	6.1499×10^{-5}	5.7229×10^{-5}	5.3588×10^{-5}	5.0488×10^{-5}
12	2.9095×10^{-5}	2.7287×10^{-5}	2.5693×10^{-5}	2.4289×10^{-5}	2.3052×10^{-5}	2.1965×10^{-5}	2.1010×10^{-5}
14	1.2794×10^{-5}	1.2190×10^{-5}	1.1646×10^{-5}	1.1157×10^{-5}	1.0717×10^{-5}	1.0323×10^{-5}	9.9699×10^{-6}
16	6.3614×10^{-6}	6.1235×10^{-6}	5.9062×10^{-6}	5.7079×10^{-6}	5.5272×10^{-6}	5.3627×10^{-6}	5.2134×10^{-6}
18	3.4599×10^{-6}	3.3541×10^{-6}	3.2565×10^{-6}	3.1666×10^{-6}	3.0837×10^{-6}	3.0075×10^{-6}	2.9376×10^{-6}
20	2.0155×10^{-6}	1.9640×10^{-6}	1.9160×10^{-6}	1.8714×10^{-6}	1.8301×10^{-6}	1.7918×10^{-6}	1.7563×10^{-6}
22	1.2397×10^{-6}	1.2127×10^{-6}	1.1874×10^{-6}	1.1637×10^{-6}	1.1416×10^{-6}	1.1210×10^{-6}	1.1018×10^{-6}
24	7.9701×10^{-7}	7.8197×10^{-7}	7.6782×10^{-7}	7.5452×10^{-7}	7.4204×10^{-7}	7.3033×10^{-7}	7.1938×10^{-7}
26	5.3155×10^{-7}	5.2276×10^{-7}	5.1445×10^{-7}	5.0661×10^{-7}	4.9922×10^{-7}	4.9227×10^{-7}	4.8572×10^{-7}
28	3.6566×10^{-7}	3.6030×10^{-7}	3.5522×10^{-7}	3.5041×10^{-7}	3.4586×10^{-7}	3.4156×10^{-7}	3.3751×10^{-7}
30	2.5830×10^{-7}	2.5492×10^{-7}	2.5170×10^{-7}	2.4865×10^{-7}	2.4575×10^{-7}	2.4300×10^{-7}	2.4040×10^{-7}
40	6.0949×10^{-8}	6.0447×10^{-8}	5.9964×10^{-8}	5.9502×10^{-8}	5.9058×10^{-8}	5.8632×10^{-8}	5.8225×10^{-8}
50	1.9959×10^{-8}	1.9844×10^{-8}	1.9732×10^{-8}	1.9625×10^{-8}	1.9521×10^{-8}	1.9421×10^{-8}	1.9324×10^{-8}
60	8.0278×10^{-9}	7.9930×10^{-9}	7.9592×10^{-9}	7.9264×10^{-9}	7.8947×10^{-9}	7.8640×10^{-9}	7.8342×10^{-9}
70	3.7189×10^{-9}	3.7062×10^{-9}	3.6939×10^{-9}	3.6819×10^{-9}	3.6702×10^{-9}	3.6589×10^{-9}	3.6479×10^{-9}
80	1.9100×10^{-9}	1.9047×10^{-9}	1.8996×10^{-9}	1.8945×10^{-9}	1.8896×10^{-9}	1.8849×10^{-9}	1.8802×10^{-9}
90	1.0613×10^{-9}	1.0588×10^{-9}	1.0564×10^{-9}	1.0541×10^{-9}	1.0518×10^{-9}	1.0496×10^{-9}	1.0474×10^{-9}
100	6.2743×10^{-10}	6.2620×10^{-10}	6.2500×10^{-10}	6.2382×10^{-10}	6.2267×10^{-10}	6.2155×10^{-10}	6.2045×10^{-10}
110	3.9001×10^{-10}	3.8935×10^{-10}	3.8870×10^{-10}	3.8807×10^{-10}	3.8745×10^{-10}	3.8685×10^{-10}	3.8626×10^{-10}
120	2.5268×10^{-10}	2.5230×10^{-10}	2.5194×10^{-10}	2.5158×10^{-10}	2.5123×10^{-10}	2.5088×10^{-10}	2.5054×10^{-10}
130	1.6949×10^{-10}	1.6927×10^{-10}	1.6905×10^{-10}	1.6884×10^{-10}	1.6863×10^{-10}	1.6842×10^{-10}	1.6822×10^{-10}
140	1.1711×10^{-10}	1.1697×10^{-10}	1.1683×10^{-10}	1.1670×10^{-10}	1.1657×10^{-10}	1.1645×10^{-10}	1.1632×10^{-10}
150	8.3001×10^{-11}	8.2914×10^{-11}	8.2829×10^{-11}	8.2745×10^{-11}	8.2662×10^{-11}	8.2581×10^{-11}	8.2501×10^{-11}

The Weyl curvature component ψ_4 contains all the information regarding the gravitational radiation. Teukolsky showed that if we carry out Fourier-harmonic decomposition of $\rho^{-4}\psi_4$, we can separate the Teukolsky equation into a radial part

Table VIII. Relative error of the energy flux between Ref. 22) and our results for $r_0 = 10M, q = 0$.

ℓ	$\mid m \mid$	Tagoshi and Nakamura	This paper	Absolute values of relative error
2	1	$1.9316093511566875 \times 10^{-7}$	$1.9316093511566907 \times 10^{-7}$	1.64×10^{-15}
2	2	$5.3687954791021136 \times 10^{-5}$	$5.3687954791021361 \times 10^{-5}$	4.20×10^{-15}
3	1	$5.7148989126147667 \times 10^{-10}$	$5.7148989126147834 \times 10^{-10}$	2.91×10^{-15}
3	2	$4.7959164615902625 \times 10^{-8}$	$4.7959164615902543 \times 10^{-8}$	1.71×10^{-15}
3	3	$6.4260827562472322 \times 10^{-6}$	$6.4260827562472412 \times 10^{-6}$	1.39×10^{-15}
4	1	$1.4575856422971336 \times 10^{-13}$	$1.4575856422971290 \times 10^{-13}$	3.19×10^{-15}
4	2	$5.2622453089592304 \times 10^{-10}$	$5.2622453089592954 \times 10^{-10}$	1.24×10^{-14}
4	3	$8.7787575252149415 \times 10^{-9}$	$8.7787575252150748 \times 10^{-9}$	1.52×10^{-14}
4	4	$9.5396003948519482 \times 10^{-7}$	$9.5396003948518797 \times 10^{-7}$	7.18×10^{-15}
5	1	$2.3676371874495427 \times 10^{-16}$	$2.3676371874495484 \times 10^{-16}$	2.40×10^{-15}
5	2	$3.8193532371989606 \times 10^{-13}$	$3.8193532371989253 \times 10^{-13}$	9.24×10^{-15}
5	3	$1.8291013252282956 \times 10^{-10}$	$1.8291013252283069 \times 10^{-10}$	6.20×10^{-15}
5	4	$1.4921162748528251 \times 10^{-9}$	$1.4921162748527967 \times 10^{-9}$	1.91×10^{-14}
5	5	$1.5241547645798743 \times 10^{-7}$	$1.5241547645799033 \times 10^{-7}$	1.90×10^{-14}
6	1	$3.5977953599117842 \times 10^{-20}$	$3.5977953599117314 \times 10^{-20}$	1.47×10^{-14}
6	2	$1.9763689535200328 \times 10^{-15}$	$1.9763689535200461 \times 10^{-15}$	6.73×10^{-15}
6	3	$2.1238827476369010 \times 10^{-13}$	$2.1238827476368560 \times 10^{-13}$	2.12×10^{-14}
6	4	$4.6633398847411170 \times 10^{-11}$	$4.6633398847412050 \times 10^{-11}$	1.89×10^{-14}
6	5	$2.4746386947271652 \times 10^{-10}$	$2.4746386947272387 \times 10^{-10}$	2.97×10^{-14}
6	6	$2.5182131568101545 \times 10^{-8}$	$2.5182131568101642 \times 10^{-8}$	3.82×10^{-15}
7	1	$3.2913629491589289 \times 10^{-23}$	$3.2913629491588661 \times 10^{-23}$	1.91×10^{-14}
7	2	$9.0841508908488114 \times 10^{-19}$	$9.0841508908487538 \times 10^{-19}$	6.34×10^{-15}
7	3	$2.0373627509685863 \times 10^{-15}$	$2.0373627509686016 \times 10^{-15}$	7.53×10^{-15}
7	4	$6.9940936502071495 \times 10^{-14}$	$6.9940936502074081 \times 10^{-14}$	3.70×10^{-14}
7	5	$1.0340989127935083 \times 10^{-11}$	$1.0340989127934911 \times 10^{-11}$	1.66×10^{-14}
7	6	$4.0679948091711724 \times 10^{-11}$	$4.0679948091710895 \times 10^{-11}$	2.04×10^{-14}
7	7	$4.2345226712846746 \times 10^{-9}$	$4.2345226712847762 \times 10^{-9}$	2.40×10^{-14}

and an angular part, or

$$\rho^{-4}\psi_4(t,r,\theta,\phi) = \sum_{\ell,m}\int d\omega e^{-i\omega t+im\varphi}\ {}_{-2}S^{a\omega}_{\ell m}(\theta)R_{\ell m\omega}(r),$$

$$4\pi\Sigma\hat{T} = \sum_{\ell,m}\int d\omega e^{-i\omega t+im\varphi}\ {}_{-2}S^{a\omega}_{\ell m}(\theta)T_{\ell m\omega}(r), \tag{A·3}$$

where $\rho = (r - ia\cos\theta)^{-1}$.

The radial function $R_{lm\omega}(r)$ and the angular function ${}_{-2}S^{a\omega}_{lm}(\theta)$ satisfy the following Teukolsky equations:

$$\Delta^2\frac{d}{dr}\left(\frac{1}{\Delta}\frac{dR_{\ell m\omega}}{dr}\right) - V(r)R_{\ell m\omega} = T_{\ell m\omega}, \tag{A·4}$$

$$\left[\frac{1}{\sin\theta}\frac{d}{d\theta}\left\{\sin\theta\frac{d}{d\theta}\right\} - a^2\omega^2\sin^2\theta - \frac{(m-2\cos\theta)^2}{\sin^2\theta} + 4a\omega\cos\theta - 2 + 2ma\omega + \lambda\right]{}_{-2}S^{a\omega}_{\ell m} = 0. \tag{A·5}$$

Table IX. Relative error of the energy flux between Kennefick's results[?)] and our results for $r_0 = 3M, q = 0.998$.

ℓ	$\mid m \mid$	Kennefick	This paper	Absolute values of relative error
2	1	$6.328361227 \times 10^{-6}$	$6.3283737145864869 \times 10^{-6}$	1.97×10^{-6}
2	2	$7.335124682 \times 10^{-3}$	$7.3350910900390372 \times 10^{-3}$	4.58×10^{-6}
3	1	$3.451784675 \times 10^{-8}$	$3.4517924227877552 \times 10^{-8}$	2.24×10^{-6}
3	2	$5.645895586 \times 10^{-6}$	$5.6458902861747337 \times 10^{-6}$	9.39×10^{-7}
3	3	$2.208481088 \times 10^{-3}$	$2.2084763695700243 \times 10^{-3}$	2.14×10^{-6}
4	1	$8.842632418 \times 10^{-12}$	$8.8426341846420484 \times 10^{-12}$	2.00×10^{-7}
4	2	$9.650747825 \times 10^{-8}$	$9.6507761069096606 \times 10^{-8}$	2.93×10^{-6}
4	3	$3.157205166 \times 10^{-6}$	$3.1572084515052529 \times 10^{-6}$	1.04×10^{-6}
4	4	$7.897993006 \times 10^{-4}$	$7.8979614897263311 \times 10^{-4}$	3.99×10^{-6}
5	1	$2.226601380 \times 10^{-14}$	$2.2266003587317006 \times 10^{-14}$	4.59×10^{-7}
5	2	$7.623615371 \times 10^{-11}$	$7.6236253541558626 \times 10^{-11}$	1.31×10^{-6}
5	3	$9.637713992 \times 10^{-8}$	$9.6377094209411545 \times 10^{-8}$	4.74×10^{-7}
5	4	$1.524036288 \times 10^{-6}$	$1.5240423964556889 \times 10^{-6}$	4.01×10^{-6}
5	5	$3.044015502 \times 10^{-4}$	$3.0439980326075501 \times 10^{-4}$	5.74×10^{-6}
6	1	$3.850986300 \times 10^{-18}$	$3.8509863211419323 \times 10^{-18}$	5.49×10^{-9}
6	2	$5.736053080 \times 10^{-13}$	$5.7360410503468190 \times 10^{-13}$	2.10×10^{-6}
6	3	$1.315574802 \times 10^{-10}$	$1.3155762424734953 \times 10^{-10}$	1.09×10^{-6}
6	4	$6.788432814 \times 10^{-8}$	$6.7884404091806854 \times 10^{-8}$	1.12×10^{-6}
6	5	$6.900330654 \times 10^{-7}$	$6.9003809076206216 \times 10^{-7}$	7.28×10^{-6}
6	6	$1.219262418 \times 10^{-4}$	$1.2192534271212692 \times 10^{-4}$	7.37×10^{-6}
7	1	$5.063200000 \times 10^{-21}$	$5.0631852897823082 \times 10^{-21}$	2.91×10^{-6}
7	2	$3.106010424 \times 10^{-16}$	$3.1060171837611518 \times 10^{-16}$	2.18×10^{-6}
7	3	$1.769856886 \times 10^{-12}$	$1.7698525192439268 \times 10^{-12}$	2.47×10^{-6}
7	4	$1.284621326 \times 10^{-10}$	$1.2846205001945888 \times 10^{-10}$	6.43×10^{-7}
7	5	$4.051197224 \times 10^{-8}$	$4.0511763345368075 \times 10^{-8}$	5.16×10^{-6}
7	6	$3.023851152 \times 10^{-7}$	$3.0238471412501713 \times 10^{-7}$	1.33×10^{-6}
7	7	$4.993950576 \times 10^{-5}$	$4.9939392339609413 \times 10^{-5}$	2.27×10^{-6}

The potential is given by

$$V(r) = -\frac{K^2 + 4i(r-M)K}{\Delta} + 8i\omega r + \lambda, \tag{A·6}$$

where $K = (r^2+a^2)\omega - ma$ and λ is the eigenvalue of ${}_{-2}S^{a\omega}_{\ell m}(\theta)$. The angular function ${}_{-2}S^{a\omega}_{\ell m}(\theta)$ is called a spin-weighted spheroidal harmonic with spin weight -2. It is usually normalized as

$$\int_0^\pi \mid {}_{-2}S^{a\omega}_{\ell m}|^2 \sin\theta d\theta = 1. \tag{A·7}$$

In the case of a Kerr black hole, analytic form of the spin-weighted spheroidal harmonics and the eigenvalue λ are not known. However, in the case of a Schwarzschild black hole, the spin-weighted spheroidal harmonics reduce to the spin-weighted spherical harmonics, and its eigenvalue is $\lambda = \ell(\ell+1) - s(s+1)$.[33)]

We solve the radial Teukolsky equation using the Green function method. For this purpose, we introduce two kinds of the homogeneous solutions of the radial

Teukolsky equation,

$$R^{\rm in}_{lm\omega} \to \begin{cases} B^{\rm trans}_{lm\omega}\Delta^2 e^{-ikr*} & \text{for } r \to r_+, \\ r^3 B^{\rm ref}_{lm\omega} e^{i\omega r*} + r^{-1} B^{\rm inc}_{lm\omega} e^{-i\omega r*} & \text{for } r \to +\infty, \end{cases} \tag{A·8}$$

$$R^{\rm up}_{lm\omega} \to \begin{cases} C^{\rm up}_{lm\omega} e^{ikr*} + \Delta^2 C^{\rm ref}_{lm\omega} e^{-ikr*} & \text{for } r \to r_+, \\ r^3 C^{\rm trans}_{lm\omega} e^{i\omega r*} & \text{for } r \to +\infty, \end{cases} \tag{A·9}$$

where $k = \omega - ma/2Mr_+$ and r^* is the tortoise coordinate defined by

$$\begin{aligned} r^* &= \int \frac{dr^*}{dr} dr, \\ &= \int \frac{r^2 + a^2}{\Delta} dr, \\ &= r + \frac{2Mr_+}{r_+ - r_-} \ln \frac{r - r_+}{2M} - \frac{2Mr_-}{r_+ - r_-} \ln \frac{r - r_-}{2M}. \end{aligned} \tag{A·10}$$

Here $r_\pm = M \pm \sqrt{M^2 - a^2}$.

Then, a solution of the radial Teukolsky equation that is ingoing at the horizon and outgoing at the infinity can be written as

$$\begin{aligned} R_{\ell m\omega}(r) = \frac{1}{W_{lm\omega}} \Bigg\{ & R^{\rm up}_{\ell m\omega}(r) \int_{r_+}^{r} dr' \frac{T_{\ell m\omega}(r') R^{\rm in}_{\ell m\omega}(r')}{\Delta^2(r')} \\ & + R^{\rm in}_{\ell m\omega}(r) \int_{r}^{\infty} dr' \frac{T_{\ell m\omega}(r') R^{\rm up}_{\ell m\omega}(r')}{\Delta^2(r')} \Bigg\}, \end{aligned}$$

where $W_{lm\omega}$ is the Wronskian given by

$$W_{\ell m\omega} = W[\Delta^{-1/2} R^{\rm in}_{\ell m\omega}, \Delta^{-1/2} R^{\rm up}_{\ell m\omega}] = 2i\omega C^{\rm trans}_{\ell m\omega} B^{\rm inc}_{\ell m\omega}. \tag{A·11}$$

The asymptotic behavior at the horizon is given by

$$\begin{aligned} R_{\ell m\omega}(r \to r_+) &\to \frac{B^{\rm trans}_{\ell m\omega}\Delta^2 e^{-ikr^*}}{2i\omega C^{\rm trans}_{\ell m\omega} B^{\rm inc}_{\ell m\omega}} \int_{r_+}^{\infty} dr' \frac{T_{\ell m\omega}(r') R^{\rm up}_{\ell m\omega}(r')}{\Delta^2(r')} \\ &\equiv \tilde{Z}^{\rm H}_{\ell m\omega} \Delta^2 e^{-ikr^*}. \end{aligned} \tag{A·12}$$

The asymptotic behavior at infinity is given by

$$R_{\ell m\omega}(r \to \infty) \to \frac{r^3 e^{i\omega r^*}}{2i\omega B^{\rm inc}_{\ell m\omega}} \int_{r_+}^{\infty} dr' \frac{T_{\ell m\omega}(r') R^{\rm in}_{\ell m\omega}(r')}{\Delta^2(r')} \equiv \tilde{Z}^{\infty}_{\ell m\omega} r^3 e^{i\omega r^*}. \tag{A·13}$$

In this paper, we focus on the gravitational wave flux from a point particle in circular, equatorial orbits around a Kerr black hole. In this case, $\tilde{Z}_{lm\omega}$ in Eq. (A·13) takes the form

$$\tilde{Z}^{\infty}_{lm\omega} = \sum_n \delta(\omega - \omega_n) Z^{\infty}_{lm\omega_n}, \tag{A·14}$$

where $\omega_n = mM^{1/2}/(r^{3/2} + aM^{1/2})$.

Then, the time-averaged flux (luminosity) radiated to infinity is given by

$$\frac{dE}{dt} = \sum_{l,m,n} \frac{|\, Z^{\infty}_{lm\omega_n} \,|^2}{4\pi\omega_n^2}. \tag{A·15}$$

A.2. *Source term*

The source term of the Teukolsky equation, Eq. (A·4), is given by

$$T_{\ell m\omega} = 4\int d\Omega dt \rho^{-5}\bar{\rho}^{-1}(B_2' + B_2'^{*})e^{-im\varphi+i\omega t}\frac{{}_{-2}S_{\ell m}^{a\omega}}{\sqrt{2\pi}}, \tag{A·16}$$

where B_2' and B_2^* are given by

$$\begin{aligned}
B_2' &= -\frac{1}{2}\rho^8\bar{\rho}L_{-1}[\rho^{-4}L_0(\rho^{-2}\bar{\rho}^{-1}T_{nn})] \\
&\quad - \frac{1}{2\sqrt{2}}\rho^8\bar{\rho}\Delta^2 L_{-1}[\rho^{-4}\bar{\rho}^2 J_+(\rho^{-2}\bar{\rho}^{-2}\Delta^{-1}T_{\bar{m}n})], \\
B_2'^{*} &= -\frac{1}{4}\rho^8\bar{\rho}\Delta^2 J_+[\rho^{-4}J_+(\rho^{-2}\bar{\rho}T_{\bar{m}\bar{m}})] \\
&\quad - \frac{1}{2\sqrt{2}}\rho^8\bar{\rho}\Delta^2 J_+[\rho^{-4}\bar{\rho}^2\Delta^{-1}L_{-1}(\rho^{-2}\bar{\rho}^{-2}T_{\bar{m}n})] \,,
\end{aligned} \tag{A·17}$$

$$\mathcal{L}_s = \partial_\theta + \frac{m}{\sin\theta} - a\omega\sin\theta + s\cot\theta, \tag{A·18}$$

$$J_+ = \partial_r + iK/\Delta \;;\quad K = (r^2+a^2)\omega - ma,$$

and T_{nn}, $T_{\overline{m}n}$, $T_{\overline{m}\overline{m}}$ are the tetrad components of the energy momentum tensor ($T_{nn} = T_{\mu\nu}n^\mu n^\nu$ etc.). Here the bar denotes the complex conjugation.

We consider $T_{\mu\nu}$ of a monopole particle of mass μ. In this case, the energy momentum tensor takes the form

$$\begin{aligned}
T^{\mu\nu} &= \mu\int d\tau \frac{d\,z^\mu}{d\tau}\frac{d\,z^\nu}{d\tau}\frac{\delta^{(4)}(x-z(\tau))}{\sqrt{-g}}, \\
&= \mu\frac{u^\mu u^\nu}{\Sigma\sin\theta u^t}\delta(r-r(t))\delta(\theta-\theta(t))\delta(\phi-\phi(t)) \,,
\end{aligned}$$

where $u^\mu = dz^\mu/d\tau$ and $z^\mu = (t, r(t), \theta(t), \phi(t))$ is a geodesic trajectory and $\tau = \tau(t)$ is the proper time along this geodesic. The geodesic equations in the Kerr geometry are given by

$$\begin{aligned}
\Sigma\frac{dt}{d\tau} &= \frac{r^2+a^2}{\Delta}\left[E(r^2+a^2) - aL_z\right] - a\left[aE\sin^2\theta - L_z\right], \\
\Sigma\frac{dr}{d\tau} &= \pm\sqrt{R}, \\
\Sigma\frac{d\theta}{d\tau} &= \pm\sqrt{\Theta}, \\
\Sigma\frac{d\phi}{d\tau} &= \frac{a}{\Delta}\left[E(r^2+a^2) - aL_z\right] - aE + \frac{L_z}{\sin^2\theta},
\end{aligned} \tag{A·19}$$

where E and L_z are the energy and the z-component of the angular momentum of a test particle, respectively. Also, we have

$$\begin{aligned}
R &= \left[(r^2+a^2)E - aL_z\right]^2 - \Delta[r^2 + (L_z - aE)^2 + C], \\
\Theta &= C - \left[(1-E^2)a^2 + \frac{L_z^2}{\sin^2\theta}\right]\cos^2\theta,
\end{aligned}$$

where C is the Carter constant of a test particle. Note that E, L_z and C are measured in units of μ. If they are expressed in the standard units, E, L_z and C in the above equations must be replaced by E/μ, L_z/μ and C/μ^2.

Using Eq. (A·19), we obtain the tetrad components of the energy momentum tensor as

$$T_{nn} = \mu \frac{C_{nn}}{\sin\theta}\delta(r - r(t))\delta(\theta - \theta(t))\delta(\phi - \phi(t)), \tag{A·20}$$

$$T_{\bar{m}n} = \mu \frac{C_{\bar{m}n}}{\sin\theta}\delta(r - r(t))\delta(\theta - \theta(t))\delta(\phi - \phi(t)), \tag{A·21}$$

$$T_{\bar{m}\bar{m}} = \mu \frac{C_{\bar{m}\bar{m}}}{\sin\theta}\delta(r - r(t))\delta(\theta - \theta(t))\delta(\phi - \phi(t)) \,, \tag{A·22}$$

where

$$\begin{aligned}
C_{nn} &= \frac{1}{4\Sigma^3 u^{\mathrm{t}}}\left[E(r^2+a^2) - aL_z + \Sigma\frac{dr}{d\tau}\right]^2, \\
C_{\bar{m}n} &= -\frac{\rho}{2\sqrt{2}\Sigma^2 u^{\mathrm{t}}}\left[E(r^2+a^2) - aL_z + \Sigma\frac{dr}{d\tau}\right]\left[i\sin\theta\Big(aE - \frac{L_z}{\sin^2\theta}\Big) + \Sigma\frac{d\theta}{d\tau}\right], \\
C_{\bar{m}\bar{m}} &= \frac{\rho^2}{2\Sigma u^{\mathrm{t}}}\left[i\sin\theta\Big(aE - \frac{L_z}{\sin^2\theta}\Big) + \Sigma\frac{d\theta}{d\tau}\right]^2 .
\end{aligned} \tag{A·23}$$

Substituting Eq. (A·17) into Eq. (A·16) and performing integration by parts, we obtain

$$\begin{aligned}
T_{\ell m\omega} = \frac{4\mu}{\sqrt{2\pi}}\int_{-\infty}^{\infty} dt \int_0^{\pi} d\theta e^{i\omega t - im\varphi(t)} \\
\times \Big[-\frac{1}{2}L_1^{\dagger}\big\{\rho^{-4}L_2^{\dagger}(\rho^3 S_{\ell m}^{a\omega})\big\}C_{nn}\rho^{-2}\bar{\rho}^{-1}\delta(r-r(t))\delta(\theta-\theta(t)) \\
+ \frac{\Delta^2\bar{\rho}^2}{\sqrt{2}\rho}\big(L_2^{\dagger}S_{\ell m}^{a\omega} + ia(\bar{\rho}-\rho)\sin\theta S_{\ell m}^{a\omega}\big) \\
\times J_+\big\{C_{\bar{m}n}\rho^{-2}\bar{\rho}^{-2}\Delta^{-1}\delta(r-r(t))\delta(\theta-\theta(t))\big\} \\
+ \frac{1}{2\sqrt{2}}L_2^{\dagger}\big\{\rho^3 S_{\ell m}^{a\omega}(\bar{\rho}^2\rho^{-4})_{,r}\big\}C_{\bar{m}n}\Delta\rho^{-2}\bar{\rho}^{-2}\delta(r-r(t))\delta(\theta-\theta(t)) \\
- \frac{1}{4}\rho^3\Delta^2 S_{\ell m}^{a\omega}J_+\big\{\rho^{-4}J_+\big(\bar{\rho}\rho^{-2}C_{\bar{m}\bar{m}}\delta(r-r(t))\delta(\theta-\theta(t))\big)\big\}\Big],
\end{aligned} \tag{A·24}$$

where

$$\mathcal{L}_s^{\dagger} = \partial_\theta - \frac{m}{\sin\theta} + a\omega\sin\theta + s\cot\theta \,, \tag{A·25}$$

and $S_{\ell m}^{a\omega}$ denotes ${}_{-2}S_{\ell m}^{a\omega}(\theta)$ for simplicity.

The integration over θ can be performed directly. It yields

$$\begin{aligned}
T_{\ell m\omega} = \mu\int_{-\infty}^{\infty} dt e^{i\omega t - im\varphi(t)}\Delta^2\Big[(A_{nn0} + A_{\bar{m}n0} + A_{\bar{m}\bar{m}0})\delta(r-r(t)) \\
+ \{(A_{\bar{m}n1} + A_{\bar{m}\bar{m}1})\delta(r-r(t))\}_{,r} + \{A_{\bar{m}\bar{m}2}\delta(r-r(t))\}_{,rr}\Big]_{\theta=\theta(t)} \,,
\end{aligned} \tag{A·26}$$

where

$$A_{nn0} = \frac{-2}{\sqrt{2\pi}\Delta^2} C_{nn} \rho^{-2} \bar{\rho}^{-1} L_1^+ \{\rho^{-4} L_2^+ (\rho^3 S_{\ell m}^{a\omega})\}, \tag{A·27}$$

$$A_{\bar{m}n0} = \frac{2}{\sqrt{\pi}\Delta} C_{\bar{m}n} \rho^{-3} \Big[\big(L_2^+ S_{\ell m}^{a\omega}\big) \Big(\frac{iK}{\Delta} + \rho + \bar{\rho} \Big) - a \sin\theta(t) S_{\ell m}^{a\omega} \frac{K}{\Delta} (\bar{\rho} - \rho) \Big], \tag{A·28}$$

$$A_{\bar{m}\bar{m}0} = -\frac{1}{\sqrt{2\pi}} \rho^{-3} \bar{\rho} C_{\bar{m}\bar{m}} S_{\ell m}^{a\omega} \Big[-i \Big(\frac{K}{\Delta} \Big)_{,r} - \frac{K^2}{\Delta^2} + 2i\rho \frac{K}{\Delta} \Big], \tag{A·29}$$

$$A_{\bar{m}\, n\, 1} = \frac{2}{\sqrt{\pi}\Delta} \rho^{-3} C_{\bar{m}n} [L_2^+ S_{\ell m}^{a\omega} + ia \sin\theta(t) (\bar{\rho} - \rho) S_{\ell m}^{a\omega}], \tag{A·30}$$

$$A_{\bar{m}\bar{m}1} = -\frac{2}{\sqrt{2\pi}} \rho^{-3} \bar{\rho} C_{\bar{m}\bar{m}} S_{\ell m}^{a\omega} \Big(i \frac{K}{\Delta} + \rho \Big), \tag{A·31}$$

$$A_{\bar{m}\bar{m}2} = -\frac{1}{\sqrt{2\pi}} \rho^{-3} \bar{\rho} C_{\bar{m}\bar{m}} S_{\ell m}^{a\omega}. \tag{A·32}$$

Inserting Eq. (A·26) into Eqs. (A·12) and (A·13), we obtain $Z_{\ell m\omega}^{\infty,H}$ as

$$Z_{\ell m\omega}^{H} = \frac{\mu B_{lm\omega}^{\rm trans}}{2i\omega C_{lm\omega}^{\rm trans} B_{lm\omega}^{\rm inc}} \int_{-\infty}^{\infty} dt e^{i\omega t - im\varphi(t)} \mathcal{I}_{\ell m\omega}^{H}(r(t), \theta(t)) \,, \tag{A·33}$$

$$Z_{\ell m\omega}^{\infty} = \frac{\mu}{2i\omega B_{lm\omega}^{\rm inc}} \int_{-\infty}^{\infty} dt e^{i\omega t - im\varphi(t)} \mathcal{I}_{\ell m\omega}^{\infty}(r(t), \theta(t)) \,, \tag{A·34}$$

where

$$\mathcal{I}_{\ell m\omega}^{\rm H} = \Big[R_{\ell m\omega}^{\rm up} \{A_{nn0} + A_{\bar{m}n0} + A_{\bar{m}\,\bar{m}\,0}\} - \frac{dR_{\ell m\omega}^{\rm up}}{dr} \{A_{\bar{m}n1} + A_{\bar{m}\bar{m}1}\} + \frac{d^2 R_{\ell m\omega}^{\rm up}}{dr^2} A_{\bar{m}\bar{m}2} \Big]_{r=r(t),\theta=\theta(t)} \,, \tag{A·35}$$

$$\mathcal{I}_{\ell m\omega}^{\infty} = \Big[R_{\ell m\omega}^{\rm in} \{A_{nn0} + A_{\bar{m}n0} + A_{\bar{m}\bar{m}0}\} - \frac{dR_{\ell m\omega}^{\rm in}}{dr} \{A_{\bar{m}n1} + A_{\bar{m}\bar{m}1}\} + \frac{d^2 R_{\ell m\omega}^{\rm in}}{dr^2} A_{\bar{m}\bar{m}2} \Big]_{r=r(t),\theta=\theta(t)} \,. \tag{A·36}$$

Appendix B
—— *The Spin-Weighted Spheroidal Harmonics* ——

In this section, we review the formalism to represent the spin-weighted spheroidal harmonics in a series of Jacobi polynomials based on Ref. 34). We also discuss a method to implement this formalism in the numerical computation.

We first transform the angular Teukolsky equation as

$$\left[(1-x^2) \frac{d^2}{dx^2} - 2x \frac{d}{dx} + \xi^2 x^2 - \frac{m^2 + s^2 + 2msx}{1-x^2} - 2s\xi x + E \right] {}_sS_{lm}^{a\omega}(x) = 0, \tag{B·1}$$

where $\xi = a\,\omega, x = \cos\theta$ and $E = \lambda + s(s+1) - a^2\omega^2 + 2\,a\,m\,\omega$.

The angular function ${}_sS_{lm}^{a\omega}(x)$ is called the spin-weighted spheroidal harmonics. Equation (B·1) is a Sturm-Liouville type eigenvalue equation with the boundary conditions of the regularity at $x = \pm 1$. The eigenvalue E depends on ℓ for fixed parameters s, m and $a\omega$. Therefore we express the eigenvalue as ${}_sE_l^m(\xi)$. When $a\omega = 0$, ${}_sS_{lm}^{a\omega}(x)$ is reduced to the spin-weighted spherical harmonics, and the eigenvalue ${}_sE_l^m(\xi)$ becomes $l(l+1)$.[33)]

The differential equation Eq. (B·1) has singularities at $x = \pm 1$ and ∞. We transform the angular function as

$$ {}_sS_{lm}^{a\omega}(x) = e^{\xi x}\left(\frac{1-x}{2}\right)^{\frac{\alpha}{2}}\left(\frac{1+x}{2}\right)^{\frac{\beta}{2}}\,{}_sU_{lm}(x), \tag{B·2}$$

where $\alpha = |m+s|$ and $\beta = |m-s|$. Then, Eq. (B·1) becomes

$$\begin{aligned}
&(1-x^2)\,{}_sU_{lm}''(x) + [\beta - \alpha - (2+\alpha+\beta)x]\,{}_sU_{lm}'(x) \\
&\quad + \left[{}_sE_l^m(\xi) - \frac{\alpha+\beta}{2}\left(\frac{\alpha+\beta}{2}+1\right)\right]{}_sU_{lm}(x) \\
&\quad = \xi\left[-2(1-x^2)\,{}_sU_{lm}'(x) + (\alpha+\beta+2s+2)x\,{}_sU_{lm}(x)\right. \\
&\qquad \left. -(\xi+\beta-\alpha)\,{}_sU_{lm}(x)\right].
\end{aligned} \tag{B·3}$$

When $\xi = 0$, the right-hand side of Eq. (B·3) is zero, while the left-hand side becomes the differential equation satisfied by the Jacobi polynomials,

$$\begin{aligned}
&(1-x^2)\,P_r^{(\alpha,\beta)\prime\prime}(x) + [\beta - \alpha - (\alpha+\beta+2)x]\,P_r^{(\alpha,\beta)\prime}(x) \\
&\quad + r(r+\alpha+\beta+1)\,P_r^{(\alpha,\beta)}(x) = 0.
\end{aligned} \tag{B·4}$$

In this limit, the eigenvalue ${}_sE_\ell^m$ in the equation (B·3) becomes $\ell(\ell+1)$, where $\ell = r + (\alpha+\beta)/2 = r + \max(|\,m\,|, |\,s\,|)$.

In this paper, we use the Jacobi polynomials defined using the Rodrigue's formula by

$$P_n^{(\alpha,\beta)}(x) = \frac{(-1)^n}{2^n\,n!}(1-x)^{-\alpha}(1+x)^{-\beta}\left(\frac{d}{dx}\right)^n\left[(1-x)^{\alpha+n}(1+x)^{\beta+n}\right]. \tag{B·5}$$

Now, we expand ${}_sU_{lm}(x)$ in a series of Jacobi polynomials:

$${}_sU_{lm}(x) = \sum_{n=0}^{\infty}{}_sA_{lm}^{(n)}(\xi)\,P_n^{(\alpha,\beta)}(x). \tag{B·6}$$

The expansion coefficients ${}_sA_{lm}^{(n)}(\xi)$ satisfy the recurrence relations

$$\alpha^{(0)}\,{}_sA_{lm}^{(1)}(\xi) + \beta^{(0)}\,{}_sA_{lm}^{(0)}(\xi) = 0, \tag{B·7}$$

$$\alpha^{(n)}\,{}_sA_{lm}^{(n+1)}(\xi) + \beta^{(n)}\,{}_sA_{lm}^{(n)}(\xi) + \gamma^{(n)}\,{}_sA_{lm}^{(n-1)}(\xi) = 0, \quad (n \geq 1) \tag{B·8}$$

where

$$\alpha^{(n)} = \frac{4\xi(n+\alpha+1)(n+\beta+1)(n+(\alpha+\beta)/2+1-s)}{(2n+\alpha+\beta+2)(2n+\alpha+\beta+3)},$$
$$\beta^{(n)} = {}_sE_l^m(\xi) + \xi^2 - \left(n+\frac{\alpha+\beta}{2}\right)\left(n+\frac{\alpha+\beta}{2}+1\right) + \frac{2\xi s(\alpha-\beta)(\alpha+\beta)}{(2n+\alpha+\beta)(2n+\alpha+\beta+2)},$$
$$\gamma^{(n)} = -\frac{4\xi n(n+\alpha+\beta)(n+(\alpha+\beta)/2+s)}{(2n+\alpha+\beta-1)(2n+\alpha+\beta)}. \tag{B·9}$$

The method to determine the eigenvalue ${}_sE_l^m$ is similar to that in the case of renormalized angular momentum presented in §3.2. The three-term recurrence relation Eq. (B·8) has two independent solutions, which behave for large n as

$$A_{(1)}^{(n)} \sim \frac{\mathrm{const}(-\xi)^n}{\Gamma(n+(\alpha+\beta+3)/2-s)}, \tag{B·10}$$
$$A_{(2)}^{(n)} \sim \mathrm{const}\xi^n\Gamma(n+(\alpha+\beta+1)/2+s). \tag{B·11}$$

The first one, $A_{(1)}^{(n)}$, is the minimal solution, and the second one, $A_{(2)}^{(n)}$, is a dominant solution, since $\lim_{n\to\infty} A_{(1)}^{(n)}/A_{(2)}^{(n)} = 0$. For the case of $A_{(2)}^{(n)}$, these coefficients increase with n, and the series Eq. (B·6) diverges for all values of x. In the case of $A_{(1)}^{(n)}$, this series converges. Thus, we have to choose $A_{(1)}^{(n)}$ in the series expansion Eq. (B·6).

Next, we introduce the following:

$$R_n \equiv \frac{A_{(1)}^n}{A_{(1)}^{n-1}}, \quad L_n \equiv \frac{A_{(1)}^n}{A_{(1)}^{n+1}}. \tag{B·12}$$

The ratio R_n can be expressed as a continued fraction:

$$R_n = \frac{A_{(1)}^{(n)}}{A_{(1)}^{(n-1)}} = -\frac{\gamma^{(n)}}{\beta^{(n)}-}\frac{\alpha^{(n)}\gamma^{(n+1)}}{\beta^{(n+1)}-}\frac{\alpha^{(n+1)}\gamma^{(n+2)}}{\beta^{(n+2)}-}\cdots. \tag{B·13}$$

We can also express L_n as a continued fraction:

$$L_n = -\frac{\alpha^{(n)}}{\beta^{(n)}+\gamma^{(n)}L_{n-1}} = -\frac{\alpha^{(n)}}{\beta^{(n)}-}\frac{\alpha^{(n-1)}\gamma^{(n)}}{\beta^{(n-1)}-}\frac{\alpha^{(n-2)}\gamma^{(n-1)}}{\beta^{(n-2)}-}\cdots\frac{\alpha^{(1)}\gamma^{(2)}}{\beta^{(1)}-}\frac{\alpha^{(0)}\gamma^{(1)}}{\beta^{(0)}}. \tag{B·14}$$

This expression for R_n is valid if the continued fraction converges. By using the properties of the three-term recurrence relations (Ref. 29), p. 35), it is proved that the continued fractions Eq. (B·13) converge as long as the eigenvalue ${}_sE_l^m$ is finite.

Now, we divide Eq. (B·8) by the expansion coefficients ${}_sA_{lm}^{(n)}$ and obtain

$$h({}_sE_\ell^m) \equiv \beta^{(n)} + \alpha^{(n)} R_{n+1} + \gamma^{(n)} L_{n-1} = 0. \tag{B·15}$$

We replace R_{n+1} and L_{n-1} by the continued fractions given in Eqs. (B·13) and (B·14). We can determine the eigenvalue ${}_sE_\ell^m$ as a root of the equation Eq. (B·15), where $l = n + (\alpha + \beta)/2$. Because the equations in Eq. (B·15) with different values of n are independent, they give different values of ${}_sE_\ell^m$. We thus obtain each ${}_sE_\ell^m$ for different ℓ even if the recurrence relation Eq. (B·8) does not contain ℓ explicitly.

As in §3.2, we adopt Brent's algorithm[31] in order to determine ${}_sE_\ell^m$. In the case that $a\omega$ is not large, we can use an analytical expression of ${}_sE_\ell^m$ as the initial value of the root search algorithm. An analytical expression of ${}_sE_\ell^m$ in a series of powers of $\xi = a\omega$ is given by

$${}_sE_\ell^m = \ell(\ell+1) - \frac{2s^2 m}{\ell(\ell+1)}\xi + \left[H(\ell+1) - H(\ell) - 1\right]\xi^2 + O(\xi^3), \tag{B·16}$$

where

$$H(\ell) = \frac{2(\ell^2 - m^2)(\ell^2 - s^2)^2}{(2\ell-1)\ell^3(2\ell+1)}. \tag{B·17}$$

The function $h({}_sE_\ell^m)$ is usually monotonic, and therefore it is very easy to find the root of Eq. (B·15).

After we obtain the eigenvalue ${}_sE_\ell^m$, we can determine all the coefficients. The coefficient for $n = n_\ell = l - (\alpha+\beta)/2$ is usually the largest term. The ratio of other terms to those for $n = n_\ell$, i.e. $A_{(1)}^{(n)}/A_{(1)}^{(n_\ell)}$, can be determined using Eqs. (B·13) and (B·14) from $n = n_\ell$ to $n = 0$ or $n = \infty$.

The factor $A_{(1)}^{(n_\ell)}$ is determined by the normalization condition. For this, we introduce a new function ${}_sV_{lm}(x)$ through

$${}_sS_{lm}^{a\omega}(x) = e^{-\xi x}\left(\frac{1-x}{2}\right)^{\frac{\alpha}{2}}\left(\frac{1+x}{2}\right)^{\frac{\beta}{2}} {}_sV_{lm}(x). \tag{B·18}$$

From Eqs. (B·2) and (B·18), we find

$${}_sV_{lm}(x) = \exp(2\xi x)\, {}_sU_{lm}(x). \tag{B·19}$$

We insert Eq. (B·18) into Eq. (B·1) and find that ${}_sV_{lm}(x)$ satisfies the differential equation

$$\begin{aligned}
&(1-x^2)\, {}_sV_{lm}''(x) + \left[\beta - \alpha - (2+\alpha+\beta)x\right] {}_sV_{lm}'(x) \\
&\quad + \left[{}_sE_l^m(\xi) - \frac{\alpha+\beta}{2}\left(\frac{\alpha+\beta}{2}+1\right)\right] {}_sV_{lm}(x) \\
&= \xi\left[2(1-x^2)\, {}_sV_{lm}'(x) - (\alpha+\beta-2s+2)x\, {}_sV_{lm}(x)\right. \\
&\quad \left. -(\xi - \beta + \alpha)\, {}_sV_{lm}(x)\right].
\end{aligned} \tag{B·20}$$

In the same way as in the case of ${}_sU_{lm}(x)$, we expand ${}_sV_{lm}(x)$ in a series of Jacobi polynomials:

$$ {}_sV_{lm}(x) = \sum_{n=0}^{\infty} {}_sB_{lm}^{(n)}\, P_n^{(\alpha,\beta)}(x). \tag{B·21} $$

The expansion coefficients ${}_sB_{lm}^{(n)}(\xi)$ satisfy the recurrence relations

$$ \begin{aligned} \tilde{\alpha}^{(0)}\, {}_sB_{lm}^{(1)}(\xi) + \tilde{\beta}^{(0)}\, {}_sB_{lm}^{(0)}(\xi) &= 0, \\ \tilde{\alpha}^{(n)}\, {}_sB_{lm}^{(n+1)}(\xi) + \tilde{\beta}^{(n)}\, {}_sB_{lm}^{(n)}(\xi) + \tilde{\gamma}^{(n)}\, {}_sB_{lm}^{(n-1)}(\xi) &= 0, \quad (n \geq 1) \end{aligned} \tag{B·22} $$

where

$$ \begin{aligned} \tilde{\alpha}^{(n)} &= -\frac{4\xi(n+\alpha+1)(n+\beta+1)(n+(\alpha+\beta)/2+1+s)}{(2n+\alpha+\beta+2)(2n+\alpha+\beta+3)}, \\ \tilde{\beta}^{(n)} &= {}_sE_l^m(\xi) + \xi^2 - \left(n+\frac{\alpha+\beta}{2}\right)\left(n+\frac{\alpha+\beta}{2}+1\right) \\ &\quad + \frac{2\xi s(\alpha-\beta)(\alpha+\beta)}{(2n+\alpha+\beta)(2n+\alpha+\beta+2)}, \\ \tilde{\gamma}^{(n)} &= \frac{4\xi n(n+\alpha+\beta)(n+(\alpha+\beta)/2-s)}{(2n+\alpha+\beta-1)(2n+\alpha+\beta)}. \end{aligned} \tag{B·23} $$

In order for the series Eq. (B·21) to converge, the coefficients ${}_sB_{lm}^{(n)}$ must constitute the minimal solution of the recurrence relation Eq. (B·22). Suppose $\{B_{(1)}^{(n)}\}$ is the minimal solution. Then, we have

$$ \frac{B_{(1)}^{(n)}}{B_{(1)}^{(n-1)}} = -\frac{\tilde{\gamma}^{(n)}}{\tilde{\beta}^{(n)}{}_-}\, \frac{\tilde{\alpha}^{(n)}\tilde{\gamma}^{(n+1)}}{\tilde{\beta}^{(n+1)}{}_-}\, \frac{\tilde{\alpha}^{(n+1)}\tilde{\gamma}^{(n+2)}}{\tilde{\beta}^{(n+2)}{}_-} \cdots, \tag{B·24} $$

$$ \frac{B_{(1)}^{(n)}}{B_{(1)}^{(n+1)}} = -\frac{\tilde{\alpha}^{(n)}}{\tilde{\beta}^{(n)}{}_-}\, \frac{\tilde{\alpha}^{(n-1)}\tilde{\gamma}^{(n)}}{\tilde{\beta}^{(n-1)}{}_-}\, \frac{\tilde{\alpha}^{(n-2)}\tilde{\gamma}^{(n-1)}}{\tilde{\beta}^{(n-2)}{}_-} \cdots \frac{\tilde{\alpha}^{(1)}\tilde{\gamma}^{(2)}}{\tilde{\beta}^{(1)}{}_-}\, \frac{\tilde{\alpha}^{(0)}\tilde{\gamma}^{(1)}}{\tilde{\beta}^{(0)}}. \tag{B·25} $$

From these equations, we can determine the ratios of all the coefficients, $B_{(1)}^{(n)}/B_{(1)}^{(n_\ell)}$.

Now, we determine the value of the two coefficients $A_{(1)}^{(n_\ell)}$ and $B_{(1)}^{(n_\ell)}$. Because Eq. (B·19) must be satisfied for any value of x, we set $x = 1$ in Eq. (B·19) and obtain

$$ {}_sB_{lm}^{(n_\ell)}(\xi) \sum_{n=0}^{\infty} \frac{{}_sB_{lm}^{(n)}(\xi)}{{}_sB_{lm}^{(n_\ell)}(\xi)} \binom{n+\alpha}{n} = \exp(2\xi)\, {}_sA_{lm}^{(n_\ell)}(\xi) \sum_{n=0}^{\infty} \frac{{}_sA_{lm}^{(n)}(\xi)}{{}_sA_{lm}^{(n_\ell)}(\xi)} \binom{n+\alpha}{n}. \tag{B·26} $$

Also, from the normalization condition Eq. (A·7), we find

$$ \int_{-1}^{1} dx \left(\frac{1-x}{2}\right)^{\alpha} \left(\frac{1+x}{2}\right)^{\beta} \sum_{n_1=0}^{\infty} {}_sA_{lm}^{(n_1)} P_{n_1}^{(\alpha,\beta)}(x) \sum_{n_2=0}^{\infty} {}_sB_{lm}^{(n_2)} P_{n_2}^{(\alpha,\beta)}(x) = 1. \tag{B·27} $$

Table X. E_{lm} for $Mw = 0.1$.

ℓ	m	$q = -0.9$	$q = 0.9$
2	2	$6.2340859091 \times 10^{0}$	$5.7540002160 \times 10^{0}$
2	1	$6.1153623140 \times 10^{0}$	$5.8752937655 \times 10^{0}$
2	0	$5.9957562220 \times 10^{0}$	$5.9957562220 \times 10^{0}$
2	−1	$5.8752937655 \times 10^{0}$	$6.1153623140 \times 10^{0}$
2	−2	$5.7540002160 \times 10^{0}$	$6.2340859091 \times 10^{0}$
3	3	$1.2175986227 \times 10^{1}$	$1.1815913335 \times 10^{1}$
3	2	$1.2116698236 \times 10^{1}$	$1.1876700620 \times 10^{1}$
3	1	$1.2057141841 \times 10^{1}$	$1.1937158320 \times 10^{1}$
3	0	$1.1997300442 \times 10^{1}$	$1.1997300442 \times 10^{1}$
3	−1	$1.1937158320 \times 10^{1}$	$1.2057141841 \times 10^{1}$
3	−2	$1.1876700620 \times 10^{1}$	$1.2116698236 \times 10^{1}$
3	−3	$1.1815913335 \times 10^{1}$	$1.2175986227 \times 10^{1}$
4	4	$2.0141120497 \times 10^{1}$	$1.9853070617 \times 10^{1}$
4	3	$2.0105083654 \times 10^{1}$	$1.9889090042 \times 10^{1}$
4	2	$2.0069068104 \times 10^{1}$	$1.9925093222 \times 10^{1}$
4	1	$2.0033067556 \times 10^{1}$	$1.9961086374 \times 10^{1}$
4	0	$1.9997075735 \times 10^{1}$	$1.9997075735 \times 10^{1}$
4	−1	$1.9961086374 \times 10^{1}$	$2.0033067556 \times 10^{1}$
4	−2	$1.9925093222 \times 10^{1}$	$2.0069068104 \times 10^{1}$
4	−3	$1.9889090042 \times 10^{1}$	$2.0105083654 \times 10^{1}$
4	−4	$1.9853070617 \times 10^{1}$	$2.0141120497 \times 10^{1}$
5	5	$3.0117824408 \times 10^{1}$	$2.9877790649 \times 10^{1}$
5	4	$3.0093445069 \times 10^{1}$	$2.9901445845 \times 10^{1}$
5	3	$3.0069155402 \times 10^{1}$	$2.9925172191 \times 10^{1}$
5	2	$3.0044953129 \times 10^{1}$	$2.9948972039 \times 10^{1}$
5	1	$3.0020835961 \times 10^{1}$	$2.9972847731 \times 10^{1}$
5	0	$2.9996801598 \times 10^{1}$	$2.9996801598 \times 10^{1}$
5	−1	$2.9972847731 \times 10^{1}$	$3.0020835961 \times 10^{1}$
5	−2	$2.9948972039 \times 10^{1}$	$3.0044953129 \times 10^{1}$
5	−3	$2.9925172191 \times 10^{1}$	$3.0069155402 \times 10^{1}$
5	−4	$2.9901445845 \times 10^{1}$	$3.0093445069 \times 10^{1}$
5	−5	$2.9877790649 \times 10^{1}$	$3.0117824408 \times 10^{1}$
6	6	$4.2101144835 \times 10^{1}$	$4.1895407126 \times 10^{1}$
6	5	$4.2083478965 \times 10^{1}$	$4.1912048117 \times 10^{1}$
6	4	$4.2065910934 \times 10^{1}$	$4.1928777542 \times 10^{1}$
6	3	$4.2048439822 \times 10^{1}$	$4.1945596361 \times 10^{1}$
6	2	$4.2031064705 \times 10^{1}$	$4.1962505533 \times 10^{1}$
6	1	$4.2013784654 \times 10^{1}$	$4.1979506008 \times 10^{1}$
6	0	$4.1996598734 \times 10^{1}$	$4.1996598734 \times 10^{1}$
6	−1	$4.1979506008 \times 10^{1}$	$4.2013784654 \times 10^{1}$
6	−2	$4.1962505533 \times 10^{1}$	$4.2031064705 \times 10^{1}$
6	−3	$4.1945596361 \times 10^{1}$	$4.2048439822 \times 10^{1}$
6	−4	$4.1928777542 \times 10^{1}$	$4.2065910934 \times 10^{1}$
6	−5	$4.1912048117 \times 10^{1}$	$4.2083478965 \times 10^{1}$
6	−6	$4.1895407126 \times 10^{1}$	$4.2101144835 \times 10^{1}$

Table XI. Spin weighted spheroidal harmonics for $M\omega = 0.1$ and $\cos\theta = -0.9$.

ℓ	m	$q = -0.9$	$q = 0.9$
2	2	$4.3386981105 \times 10^{-3}$	$3.5950865567 \times 10^{-3}$
2	1	$-3.7087357243 \times 10^{-2}$	$-3.1984590567 \times 10^{-2}$
2	0	$1.9411700165 \times 10^{-1}$	$1.7424257031 \times 10^{-1}$
2	−1	$-6.7728189805 \times 10^{-1}$	$-6.3276040875 \times 10^{-1}$
2	−2	$1.4469520014 \times 10^{0}$	$1.4070158595 \times 10^{0}$
3	3	$2.6579791433 \times 10^{-3}$	$2.3432796925 \times 10^{-3}$
3	2	$-2.3106765235 \times 10^{-2}$	$-2.0900105378 \times 10^{-2}$
3	1	$1.2376650604 \times 10^{-1}$	$1.1489471197 \times 10^{-1}$
3	0	$-4.4858142218 \times 10^{-1}$	$-4.2770231715 \times 10^{-1}$
3	−1	$1.0509804998 \times 10^{0}$	$1.0312667647 \times 10^{0}$
3	−2	$-1.1695230417 \times 10^{0}$	$-1.1936637613 \times 10^{0}$
3	−3	$-9.1785502130 \times 10^{-1}$	$-8.8540840083 \times 10^{-1}$
4	4	$1.3964986285 \times 10^{-3}$	$1.2717039185 \times 10^{-3}$
4	3	$-1.2581385396 \times 10^{-2}$	$-1.1651738472 \times 10^{-2}$
4	2	$7.0862042637 \times 10^{-2}$	$6.6759828566 \times 10^{-2}$
4	1	$-2.7776127987 \times 10^{-1}$	$-2.6634215480 \times 10^{-1}$
4	0	$7.5267562259 \times 10^{-1}$	$7.3543750538 \times 10^{-1}$
4	−1	$-1.2550656615 \times 10^{0}$	$-1.2540767509 \times 10^{0}$
4	−2	$6.8973736289 \times 10^{-1}$	$7.2640111281 \times 10^{-1}$
4	−3	$1.2548549058 \times 10^{0}$	$1.2430573062 \times 10^{0}$
4	−4	$4.9003837955 \times 10^{-1}$	$4.7271311939 \times 10^{-1}$
5	5	$6.8987908263 \times 10^{-4}$	$6.4066680667 \times 10^{-4}$
5	4	$-6.4686885018 \times 10^{-3}$	$-6.0782911246 \times 10^{-3}$
5	3	$3.8436104725 \times 10^{-2}$	$3.6551010190 \times 10^{-2}$
5	2	$-1.6262489225 \times 10^{-1}$	$-1.5656422649 \times 10^{-1}$
5	1	$4.9724643493 \times 10^{-1}$	$4.8496714304 \times 10^{-1}$
5	0	$-1.0442277264 \times 10^{0}$	$-1.0333677913 \times 10^{0}$
5	−1	$1.2430710500 \times 10^{0}$	$1.2553442781 \times 10^{0}$
5	−2	$-9.9162402163 \times 10^{-2}$	$-1.3327302849 \times 10^{-1}$
5	−3	$-1.3250352372 \times 10^{0}$	$-1.3300224425 \times 10^{0}$
5	−4	$-8.7853110913 \times 10^{-1}$	$-8.6299962142 \times 10^{-1}$
5	−5	$-2.4419490099 \times 10^{-1}$	$-2.3603241859 \times 10^{-1}$
6	6	$3.2984531756 \times 10^{-4}$	$3.1033107890 \times 10^{-4}$
6	5	$-3.2192050631 \times 10^{-3}$	$-3.0549982369 \times 10^{-3}$
6	4	$2.0138768387 \times 10^{-2}$	$1.9279986867 \times 10^{-2}$
6	3	$-9.1318426706 \times 10^{-2}$	$-8.8215649196 \times 10^{-2}$
6	2	$3.0845665000 \times 10^{-1}$	$3.0079608194 \times 10^{-1}$
6	1	$-7.6021402310 \times 10^{-1}$	$-7.4896406387 \times 10^{-1}$
6	0	$1.2535400677 \times 10^{0}$	$1.2503499550 \times 10^{0}$
6	−1	$-1.0079278456 \times 10^{0}$	$-1.0282273588 \times 10^{0}$
6	−2	$-4.8304664552 \times 10^{-1}$	$-4.5779972946 \times 10^{-1}$
6	−3	$1.1370699694 \times 10^{0}$	$1.1530844521 \times 10^{0}$
6	−4	$1.1913495835 \times 10^{0}$	$1.1822538661 \times 10^{0}$
6	−5	$5.2560056636 \times 10^{-1}$	$5.1488724800 \times 10^{-1}$
6	−6	$1.1736688454 \times 10^{-1}$	$1.1371714705 \times 10^{-1}$

Table XII. Spin weighted spheroidal harmonics for $M\omega = 0.1$ and $\cos\theta = 0$.

ℓ	m	$q = -0.9$	$q = 0.9$
2	2	$4.1111211672 \times 10^{-1}$	$3.7950484443 \times 10^{-1}$
2	1	$-8.0605525927 \times 10^{-1}$	$-7.7444328043 \times 10^{-1}$
2	0	$9.6770343965 \times 10^{-1}$	$9.6770343965 \times 10^{-1}$
2	−1	$-7.7444328043 \times 10^{-1}$	$-8.0605525927 \times 10^{-1}$
2	−2	$3.7950484443 \times 10^{-1}$	$4.1111211672 \times 10^{-1}$
3	3	$5.8559507510 \times 10^{-1}$	$5.5982341302 \times 10^{-1}$
3	2	$-9.3732214203 \times 10^{-1}$	$-9.3264155844 \times 10^{-1}$
3	1	$7.1502176780 \times 10^{-1}$	$7.6307833481 \times 10^{-1}$
3	0	$3.8419145390 \times 10^{-2}$	$-3.8419145390 \times 10^{-2}$
3	−1	$-7.6307833481 \times 10^{-1}$	$-7.1502176780 \times 10^{-1}$
3	−2	$9.3264155844 \times 10^{-1}$	$9.3732214203 \times 10^{-1}$
3	−3	$-5.5982341302 \times 10^{-1}$	$-5.8559507510 \times 10^{-1}$
4	4	$7.1154532347 \times 10^{-1}$	$6.9134142570 \times 10^{-1}$
4	3	$-9.8923696324 \times 10^{-1}$	$-9.9458839545 \times 10^{-1}$
4	2	$5.0542053337 \times 10^{-1}$	$5.5505006446 \times 10^{-1}$
4	1	$4.0134847826 \times 10^{-1}$	$3.4802911340 \times 10^{-1}$
4	0	$-8.3798585128 \times 10^{-1}$	$-8.3798585128 \times 10^{-1}$
4	−1	$3.4802911340 \times 10^{-1}$	$4.0134847826 \times 10^{-1}$
4	−2	$5.5505006446 \times 10^{-1}$	$5.0542053337 \times 10^{-1}$
4	−3	$-9.9458839545 \times 10^{-1}$	$-9.8923696324 \times 10^{-1}$
4	−4	$6.9134142570 \times 10^{-1}$	$7.1154532347 \times 10^{-1}$
5	5	$8.1075684145 \times 10^{-1}$	$7.9470010304 \times 10^{-1}$
5	4	$-1.0107000628 \times 10^{0}$	$-1.0200385934 \times 10^{0}$
5	3	$3.3710130936 \times 10^{-1}$	$3.8104293488 \times 10^{-1}$
5	2	$6.0312055648 \times 10^{-1}$	$5.6888007421 \times 10^{-1}$
5	1	$-7.6566919046 \times 10^{-1}$	$-7.8489902785 \times 10^{-1}$
5	0	$-2.5485570450 \times 10^{-2}$	$2.5485570450 \times 10^{-2}$
5	−1	$7.8489902785 \times 10^{-1}$	$7.6566919046 \times 10^{-1}$
5	−2	$-5.6888007421 \times 10^{-1}$	$-6.0312055648 \times 10^{-1}$
5	−3	$-3.8104293488 \times 10^{-1}$	$-3.3710130936 \times 10^{-1}$
5	−4	$1.0200385934 \times 10^{0}$	$1.0107000628 \times 10^{0}$
5	−5	$-7.9470010304 \times 10^{-1}$	$-8.1075684145 \times 10^{-1}$
6	6	$8.9272963150 \times 10^{-1}$	$8.7970600210 \times 10^{-1}$
6	5	$-1.0179015837 \times 10^{0}$	$-1.0287597521 \times 10^{0}$
6	4	$1.9938800690 \times 10^{-1}$	$2.3714685226 \times 10^{-1}$
6	3	$7.2764306367 \times 10^{-1}$	$7.0598308423 \times 10^{-1}$
6	2	$-6.6414145769 \times 10^{-1}$	$-6.8995712931 \times 10^{-1}$
6	1	$-2.7229278396 \times 10^{-1}$	$-2.3136795981 \times 10^{-1}$
6	0	$8.1612099685 \times 10^{-1}$	$8.1612099685 \times 10^{-1}$
6	−1	$-2.3136795981 \times 10^{-1}$	$-2.7229278396 \times 10^{-1}$
6	−2	$-6.8995712931 \times 10^{-1}$	$-6.6414145769 \times 10^{-1}$
6	−3	$7.0598308423 \times 10^{-1}$	$7.2764306367 \times 10^{-1}$
6	−4	$2.3714685226 \times 10^{-1}$	$1.9938800690 \times 10^{-1}$
6	−5	$-1.0287597521 \times 10^{0}$	$-1.0179015837 \times 10^{0}$
6	−6	$8.7970600210 \times 10^{-1}$	$8.9272963150 \times 10^{-1}$

Table XIII. Spin weighted spheroidal harmonics for $M\omega = 0.1$ and $\cos\theta = 0.9$.

ℓ	m	$q = -0.9$	$q = 0.9$
2	2	$1.4070158595 \times 10^{0}$	$1.4469520014 \times 10^{0}$
2	1	$-6.3276040875 \times 10^{-1}$	$-6.7728189805 \times 10^{-1}$
2	0	$1.7424257031 \times 10^{-1}$	$1.9411700165 \times 10^{-1}$
2	−1	$-3.1984590567 \times 10^{-2}$	$-3.7087357243 \times 10^{-2}$
2	−2	$3.5950865567 \times 10^{-3}$	$4.3386981105 \times 10^{-3}$
3	3	$8.8540840083 \times 10^{-1}$	$9.1785502130 \times 10^{-1}$
3	2	$1.1936637613 \times 10^{0}$	$1.1695230417 \times 10^{0}$
3	1	$-1.0312667647 \times 10^{0}$	$-1.0509804998 \times 10^{0}$
3	0	$4.2770231715 \times 10^{-1}$	$4.4858142218 \times 10^{-1}$
3	−1	$-1.1489471197 \times 10^{-1}$	$-1.2376650604 \times 10^{-1}$
3	−2	$2.0900105378 \times 10^{-2}$	$2.3106765235 \times 10^{-2}$
3	−3	$-2.3432796925 \times 10^{-3}$	$-2.6579791433 \times 10^{-3}$
4	4	$4.7271311939 \times 10^{-1}$	$4.9003837955 \times 10^{-1}$
4	3	$1.2430573062 \times 10^{0}$	$1.2548549058 \times 10^{0}$
4	2	$7.2640111281 \times 10^{-1}$	$6.8973736289 \times 10^{-1}$
4	1	$-1.2540767509 \times 10^{0}$	$-1.2550656615 \times 10^{0}$
4	0	$7.3543750538 \times 10^{-1}$	$7.5267562259 \times 10^{-1}$
4	−1	$-2.6634215480 \times 10^{-1}$	$-2.7776127987 \times 10^{-1}$
4	−2	$6.6759828566 \times 10^{-2}$	$7.0862042637 \times 10^{-2}$
4	−3	$-1.1651738472 \times 10^{-2}$	$-1.2581385396 \times 10^{-2}$
4	−4	$1.2717039185 \times 10^{-3}$	$1.3964986285 \times 10^{-3}$
5	5	$2.3603241859 \times 10^{-1}$	$2.4419490099 \times 10^{-1}$
5	4	$8.6299962142 \times 10^{-1}$	$8.7853110913 \times 10^{-1}$
5	3	$1.3300224425 \times 10^{0}$	$1.3250352372 \times 10^{0}$
5	2	$1.3327302849 \times 10^{-1}$	$9.9162402163 \times 10^{-2}$
5	1	$-1.2553442781 \times 10^{0}$	$-1.2430710500 \times 10^{0}$
5	0	$1.0333677913 \times 10^{0}$	$1.0442277264 \times 10^{0}$
5	−1	$-4.8496714304 \times 10^{-1}$	$-4.9724643493 \times 10^{-1}$
5	−2	$1.5656422649 \times 10^{-1}$	$1.6262489225 \times 10^{-1}$
5	−3	$-3.6551010190 \times 10^{-2}$	$-3.8436104725 \times 10^{-2}$
5	−4	$6.0782911246 \times 10^{-3}$	$6.4686885018 \times 10^{-3}$
5	−5	$-6.4066680667 \times 10^{-4}$	$-6.8987908263 \times 10^{-4}$
6	6	$1.1371714705 \times 10^{-1}$	$1.1736688454 \times 10^{-1}$
6	5	$5.1488724800 \times 10^{-1}$	$5.2560056636 \times 10^{-1}$
6	4	$1.1822538661 \times 10^{0}$	$1.1913495835 \times 10^{0}$
6	3	$1.1530844521 \times 10^{0}$	$1.1370699694 \times 10^{0}$
6	2	$-4.5779972946 \times 10^{-1}$	$-4.8304664552 \times 10^{-1}$
6	1	$-1.0282273588 \times 10^{0}$	$-1.0079278456 \times 10^{0}$
6	0	$1.2503499550 \times 10^{0}$	$1.2535400677 \times 10^{0}$
6	−1	$-7.4896406387 \times 10^{-1}$	$-7.6021402310 \times 10^{-1}$
6	−2	$3.0079608194 \times 10^{-1}$	$3.0845665000 \times 10^{-1}$
6	−3	$-8.8215649196 \times 10^{-2}$	$-9.1318426706 \times 10^{-2}$
6	−4	$1.9279986867 \times 10^{-2}$	$2.0138768387 \times 10^{-2}$
6	−5	$-3.0549982369 \times 10^{-3}$	$-3.2192050631 \times 10^{-3}$
6	−6	$3.1033107890 \times 10^{-4}$	$3.2984531756 \times 10^{-4}$

Because the Jacobi polynomials are orthogonal, we have

$$\int_{-1}^{1} dx \left(\frac{1-x}{2}\right)^{\alpha} \left(\frac{1+x}{2}\right)^{\beta} P_{n_1}^{(\alpha,\beta)}(x) P_{n_2}^{(\alpha,\beta)}(x) = \frac{2\,\Gamma(n+\alpha+1)\Gamma(n+\beta+1)\delta_{n_1,n_2}}{(2n+\alpha+\beta+1)\Gamma(n+1)\Gamma(n+\alpha+\beta+1)}. \tag{B·28}$$

Then, Eq. (B·27) reduces to

$$\sum_{n=0}^{\infty} \left[\frac{{}_sA_{lm}^{(n)}}{{}_sA_{lm}^{(n_\ell)}}\right] \left[\frac{{}_sB_{lm}^{(n)}}{{}_sB_{lm}^{(n_\ell)}}\right] \frac{2\,\Gamma(n+\alpha+1)\Gamma(n+\beta+1)}{(2n+\alpha+\beta+1)\Gamma(n+1)\Gamma(n+\alpha+\beta+1)} = \frac{1}{{}_sA_{lm}^{(n_\ell)}\,{}_sB_{lm}^{(n_\ell)}}. \tag{B·29}$$

We can obtain the squares of ${}_sA_{lm}^{(n_\ell)}$ and ${}_sB_{lm}^{(n_\ell)}$ from Eqs. (B·26) and (B·29). Finally, we determine the signs of ${}_sA_{lm}^{(n_\ell)}$ and ${}_sB_{lm}^{(n_\ell)}$ by requiring that the sign of ${}_sS_{\ell m}^{a\omega}(x)$ be the same as the sign of the spin-weight spherical harmonics in the limit $a\omega \to 0$.

In Table X, we list the eigenvalues of the spin-weighted spheroidal harmonics for $q = \pm 0.9$ from $\ell = 2$ to 6 in the case $M\omega = 0.1$. In Tables XI–XIII, we list the values of the spin-weighted spheroidal harmonics for $\cos\theta = -0.9, 0, 0.9$, $q = \pm 0.9$ and $\ell = 2 - 6$.

References

1) LISA web page: `http://lisa.jpl.nasa.gov/`
2) J. R. Gair, L. Barack, T. Creighton, C. Cutler, S. L. Larson, E. S. Phinney and M. Vallisneri, gr-qc/0405137.
3) F. D. Ryan, Phys. Rev. D **52** (1995), 5707; Phys. Rev. D **56** (1997), 1845.
4) S. A. Teukolsky, Astrophys. J. **185** (1973), 635.
5) M. Sasaki and T. Nakamura, Prog. Theor. Phys. **67** (1982), 1788.
6) S. Chandrasekhar, Proc. R. Soc. London A **343** (1975), 289.
7) J. M. Bardeen and W. H. Press, J. Math. Phys. **14** (1973), 7.
8) T. Nakamura, K. Oohara and Y. Kojima, Prog. Theor. Phys. Suppl. No. 90 (1987), 1.
9) M. Shibata, Phys. Rev. D **48** (1993), 663.
10) L. S. Finn and K. S. Thorne, Phys. Rev. D **62** (2000), 124021.
11) T. Tanaka, M. Shibata, M. Sasaki, H. Tagoshi and T. Nakamura, Prog. Theor. Phys. **90** (1993), 65.
12) C. Cutler, D. Kennefick and E. Poisson, Phys. Rev. D **50** (1994), 3816.
13) T. Apostolatos, D. Kennefick, A. Ori and E. Poisson, Phys. Rev. D **47** (1993), 5376.
14) D. Kennefick, Phys. Rev. D **58** (1998), 064012.
15) M. Shibata, Phys. Rev. D **50** (1994), 6297.
16) K. Glampedakis and D. Kennefick, Phys. Rev. D **66** (2002), 044002.
17) M. Shibata, Prog. Theor. Phys. **90** (1993), 595.
18) S. A. Hughes, Phys. Rev. D **61** (2000), 084004.
19) S. A. Hughes, Phys. Rev. D **64** (2001), 064004.
20) C. Cutler, L. S. Finn, E. Poisson and G. J. Sussman, Phys. Rev. D **47** (1993), 1511.
21) E. W. Leaver, J. Math. Phys. **27** (1986), 1238.
22) H. Tagoshi and T. Nakamura, Phys. Rev. D **49** (1994), 4016.
23) S. Mano, H. Suzuki and E. Takasugi, Prog. Theor. Phys. **95** (1996), 1079.
24) Y. Mino, M. Sasaki, M. Shibata, H. Tagoshi and T. Tanaka, Prog. Theor. Phys. Suppl. No. 128 (1997), 1.
25) M. Sasaki and H. Tagoshi, Living Rev. Relativity **6** (2003), 6, `http://www.livingreviews.org/lrr-2003-6/`

26) H. Tagoshi, S. Mano and E. Takasugi, Prog. Theor. Phys. **98** (1997), 829.
27) S. Mano and E. Takasugi, Prog. Theor. Phys. **97** (1996), 213.
28) *Handbook of Mathematical Functions*, ed. M. Abramowitz and I. A. Stegun (Dover, New York, 1972).
29) W. Gautschi, S. I. A. M. Review **9** (1967), 24.
30) A. R. Barnett, D. H. Feng, J. W. Steed and L. J. B. Goldfarb, Comput. Phys. Commun. **8** (1974), 377.
31) W. H. Press, S. A. Teukolsky, W. T. Vetterling and B. P. Flannery, *Numerical Recipes in C* (Cambridge University Press, Cambridge, England, 1992).
32) T. Ooura, Online software library: `http://momonga.t.u-tokyo.ac.jp/~ooura/`
33) W. H. Press and S. A. Teukolsky, Astrophys. J. **185** (1973), 649.
34) E. D. Fackerell and R. G. Crossman, J. Math. Phys. **9** (1977), 1849.